Research Article
Journal of Smart Systems Research (JOINSSR) 2(1), 48-75, 2021
Recieved: 22-Apr-2021 Accepted: 11-Jun-2021

Dynamic behaviour of functionally graded Timoshenko beams on a four parameter linear elastic foundation due to a high speed travelling mass with variable velocities

1st İsmail ESEN ,2nd Mehmet Akif KOÇ ,3rd Mustafa EROĞLU

[1]Karabük University, Engineering Faculty, Mechanical Engineering, iesen@karabuk.edu.tr
[2]Sakarya Applied Sciences University, Technology Faculty, Mechatronics Engineering, makoc@subu.edu.tr
[3]Sakarya University, Engineering Faculty, Mechanical Engineering, mustafaeroglu@sakarya.edu.tr

ABSTRACT

This study presents a four-parameter linear basis model to analyse and control the dynamic response of an FGM Timoshenko beam exposed to the accelerating / decelerating mass using the finite element method. The dynamic effects of the foundation's mass and damping are taken into account and the foundation is assumed to consist of four parts: mass, spring, viscous damper and shear layer. Considering the actual physical neutral axis, the combined motion equations of the FGM beam-mass-base-base system are obtained by combining terms of first order shear deformation (FSDT) and mass and base interactions. In view of the resulting high-speed motion and acceleration conditions of the moving mass, some new findings are presented for both the moving load and the moving mass assumptions to highlight the differences that may be useful in the analysis of new high-speed transport applications today. Due to their effects, the frequency change of the FGM Timoshenko beam-base system is emphasized to show the main cause of the changes.

Keywords: FGM beams, mass inertia, high-speed moving mass, four-parameter linear foundation, finite element.

Fonksiyonel olarak derecelendirilmiş Timoshenko kirişlerinin değişken hızlara sahip yüksek hızlı hareketli kütle etkisi nedeniyle dört parametreli doğrusal elastik bir temel üzerindeki dinamik davranışı

ÖZ

Bu çalışma, sonlu elemanlar yöntemini kullanarak hızlanan / yavaşlayan kütle etkisi altındaki bir FGM Timoshenko kirişinin dinamik cevabını analiz etmek ve kontrol etmek için dört parametreli bir doğrusal temel model sunmaktadır. Temelin kütlesinin ve sönümlemesinin dinamik etkileri dikkate alınarak ve temelin dört bölümden oluştuğu varsayılarak: kütle, yay, viskoz sönümleyici ve kayma tabakası göz önünde bulundurulmuştur. Gerçek fiziksel nötr eksen göz önüne alındığında, FGM kiriş-kütle-taban-temel sisteminin birleşik hareket denklemleri, birinci dereceden kayma deformasyonu (FSDT) ve kütle ve taban etkileşimleri terimleri birleştirilerek elde edilmiştir. Hareketli kütlenin ortaya çıkan yüksek hızlı hareket ve ivme koşulları göz önüne alındığında, yeni yüksek hızlı taşıma uygulamalarının analizinde faydalı olabilecek farklılıkları vurgulamak için hem hareketli yük hem de hareketli kütle varsayımları için bazı yeni bulgular sunulmuştur. Etkileri nedeniyle, FGM Timoshenko kiriş-temel sisteminin frekans değişimi, değişikliklerin ana nedenini göstermek için vurgulanmıştır.

Anahtar Kelimeler: FGM kirişler, kütle ataleti, yüksek hızlı hareketli kütle, dört parametreli doğrusal temel, sonlu elemanlar.

* Corresponding Author's email:makoc@subu.edu.tr

1 Introduction

Dynamic behaviour of the structures under the influence of moving loads has been widely discussed in the literature as an important topic of interest [1–4]. Moving mass and structure interaction is also an important study subject in military applications of the mechanics, and in some studies [5–8] one can found some FEM and heuristic methods for determining muzzle displacements resulting from projectile and gun barrel interaction by considering the Coriolis, centripetal and inertia effects of the high-speed moving projectile inside the gun barrel Functionally graded materials are a new type of composite material consisting of gradual mixing of multiple materials according to a mixing law. Unlike conventional composite materials, they have superior mechanical properties with a material distribution that does not cause stress concentration. This composite material, which is composed of a mixture of metal and ceramic to obtain strength and temperature resistance, can be produced to operate under the harsh conditions of demanding aerospace, defence and space systems.

The dynamic response of supported structures on a basis is an important issue due to their widespread use in engineering applications. In particular, beams supported by foundations have an important place in structural mechanics such as the design and analysis of rails, roads and runways. Therefore, dynamic response analysis problems of beam-foundation systems under dynamic loads have attracted the attention of many researchers. [9] has examined the dynamic behaviour of sigmoid - functionally graded (S-FGM) sandwich plates on a Pasternak elastic foundation in a thermal environment. The effects of thermal media, damping and Winkler-Pasternak elastic base on the nonlinear dynamic responses of a non-nanocomposite organic solar cell (NCOSC) were investigated by [10]. Using non-local Timoshenko beam theory, the buckling of non-uniform axially functionally graded Timoshenko beams on the Winkler-Pasternak foundation has been investigated by [11]. [12] has presented the post-buckling behaviour of a thin-walled open section beam supported by the Winkler-Pasternak base due to an axial clamping load. A 3D hyperbolic theory was developed by [13] to analyse the free vibration analysis of porous (FG) plates on elastic foundations for Winkler, Pasternak and Kerr models. The nonlinear vibration and dynamic buckling of a graphene platelet-reinforced sandwich plate by the effect of thermal media, damping and Winkler-Pasternak base have been investigated by [14].

Using the von Karman strains with Reddy's HSDT, the impact analysis of Voigt model-FGM beams resting on elastic bases has been presented by [15]. The dynamic stability of an exponential law (FG) cylindrical shell encircled by the two-parameter elastic cover due to an incremental load has been analytically studied by [16] including the effect of damping. The dynamic response of (FG) truncated conical shells on the two-parameter elastic bases has been investigated by [17] using the FSTD. To eliminate the need of shear correction factors, the buckling of FG plates on elastic foundations has been presented by [18] using a hyperbolic deformation function. Using an advanced plate theory with the implementation of nonlocal elasticity, the free vibration behaviour of a FGM nanoplate supported by elastic bases has been studied by [19].

[20] has investigated the dynamic behaviour of prismatic beams on a two-parameter foundation by implementing the Timoshenko beam theory (TBT) in modelling and Runge–Kutta and Regula–Falsi methods in the numerical solutions. Using different beam theories with the modified couple stresses, [21] has studied thermo elastic dynamic response of thick microbeams encircled by elastic covers. Using thin plate theory for the nonstationary dynamics of pavements on Pasternak foundation due to accelerating loads, [22] has presented a PE-PIM method combining the power spectral density (PSD) with Duhamel's integral and a precise integration method (PIM). For four different law of the gradation, the vibration behaviour of FG carbon nanotube reinforced composite (FG-CNTRC) rectangular plates on Winkler–Pasternak foundations have been investigated by [23] using the FSTD with Navier solution. Modelling the railway ballast as a Coulomb type friction, the dynamics of an Euler-Bernoulli beam on a frictional-elastic base exposed to a uniformly moving concentrated force has been investigated by [24]. According to the TSDT in combination with the von Karman strains, the elastic deformations of FG-CNTRC variable thickness annular plates on a two-parameter base has been investigated by [25], using an analytical iterative method. Considering Reddy's HSDT and the von Karman strains for a graphene reinforced composite FG plates supported by a two parameter base in a thermal environment, [26] has studied the nonlinear vibration behaviour by adopting non local effects and extended Halpin-Tsai material model. Using Reddy's HSDT and the von Karman type kinematic nonlinearity and [27] has

studied the impact response of Voigt model temperature dependent material FG plates on an elastic base with three-parameters. [28] has proposed a new refined deformation shape in order to examining the dynamic response of a FG plate supported by an elastic base. For the free response of thick plates supported by a two-parameter elastic base, [29] has used the FSDT with the Galerkin Method. Using the direct Liapunov method, the vibration response of a Timoshenko beam on a three-parameter viscoelastic base and exposed to axial loading has been presented by [30]. Using the Fourier transformation and the Adomian methods, the vibrations of endless Timoshenko beams supported by a cubic elastic base subjected to a moving load has been studied by [31]. The dynamics of the shells on a Pasternak foundation has been studied by [32] using matrix transformation method. Using Galerkin and superposition methods, the bending of composite shells on a Pasternak foundation due to an external pressure and axial compression has been analysed by [33]. Using an analytical method, a new HSDT has been proposed by [34] for sigmoid (S), power-law (P) , and exponential (E) FGM plates supported by elastic bases. Considering the depth change of the flexural distortions of the beam-columns on the Winkler foundation, the fundamental frequencies and buckling stresses have been analysed by [35]. The vibration and stability of initially stressed beams on the Winkler foundation has been studied by [36] using the FEM.

Considering the separation which can be occur when the contact force chances its sing, [37] has investigated the vibration response of a Timoshenko beam supported by spring foundation and exposed to a moving mass, and it has shown that the possible separation in velocities of the mass can be suppressed by higher spring coefficient of the elastic foundation. Considering the various models of the soils, [38] has compared the available models in the literature. Although Winkler is one of the simplest models for defining elastic soil behavior, one of the major shortcomings of the Winkler model is the discontinuity of displacement between the loaded and unloaded parts of the surface. To overcome the lack of the Winkler model, some researchers [39–43] have proposed different foundation models to define the more real response of the soil by establishing independent mass-free springs. Under a harmonic moving force, the vibrations of an infinite Timoshenko beam on a viscoelastic base has been investigated by [44]. [45] has presented the response of a FG Timoshenko beam supported by an elastic foundation. [46] has studied the dynamics of a FG Timoshenko beam supported by an elastic base. Considering braking and acceleration of the vehicle a modelling of vehicle–bridge interaction (VBI) has been proposed by [47] using FEM, while a numerical method for VBI analysis of cars in abrupt deceleration has been studied by [48]. The dynamic response of functionally graded beams subjected to a variable speed moving load is studied by [49]. They considered only transverse effect of the load by ommiting mass inertia and axial force due to the variable speed. The dynamic response of FG beams exposed to a travelling harmonic point load has been given by [50]. [51] has presented a mixed Ritz-DQ method for the dynamics of FG beams subjected to moving loads. Considering various boundary conditions and omitting the mass inertia, some scientists [52–54] have also studied the vibrations of the beams exposed to moving loads. Some moving mass studies accounting mass inertia and variable velocity are given in [55–58]. The stress distribution in the FGMs have been studied by [59] using the FEM. Many different modelling studies of the FGMs have been widely presented by [60]. Including the FGMs, the advanced applications of materials in space and aviation have been given by [61]. The determination of the neutral plane location and its effects on the vibrations of FG beams have been studied by [62] and based on physical neutral surface, [63] has studied the vibration behaviour of FG plates. For the vibrations and buckling of regular Timoshenko beams subjected to an axial load, [64] has proposed a 6 DOF new finite element with two nodes and [65] has proposed a 6 DOF beam elemet for FGM Timoshenko beams. An orher analytical method for dynamics of FGM beams has been presented by [66].

In literature, in general, the mass of the foundation and the effect of mass on dynamic behaviour are neglected in terms of simplicity. In fact, if neglected, the foundation has a mass that moves with the superstructure, which alters the actual natural frequency and actual behaviour, which can cause errors in calculating the reliability of critical structures and cause accidents. Due to this fact, the dynamic response of structures on a foundation should be analysed considering the mass density of the base. Furthermore, the solution and analysis methods presented in the literature for FGM beams exposed to a moving mass are generally for simplified cases of convective acceleration, high speed, mass, and variable speed effects of the moving load. In this study, implementing the FEM a useful modelling of the interaction between a

variable high-speed moving load and a FGM beam supported by a four-parameter viscoelastic base is presented. With a new linear model including springs, shear layer, mass and viscous damping, the analysis of sub-base parameters on the dynamics of FGM beams due to a moving mass can be examined and optimal parameters can be defined for an accurate design.

2 Finite-element modelling

Figure 1 shows a four-parameter foundation system supporting an FGM beam under an accelerated mass effect. The new linear foundation model consists of the spring and share modules $\boldsymbol{k_S}$, $\boldsymbol{k_G}$, and a mass $\boldsymbol{m_f}$ and a viscous damping coefficient $\boldsymbol{c_f}$. For the continuous contact of the moving mass and the beam, the symbol x_p describes the global location, while x_m stands for the location on the beam element s. The beam is of a uniform cross-section and the material is distributed in thickness direction in accordance with a power law.

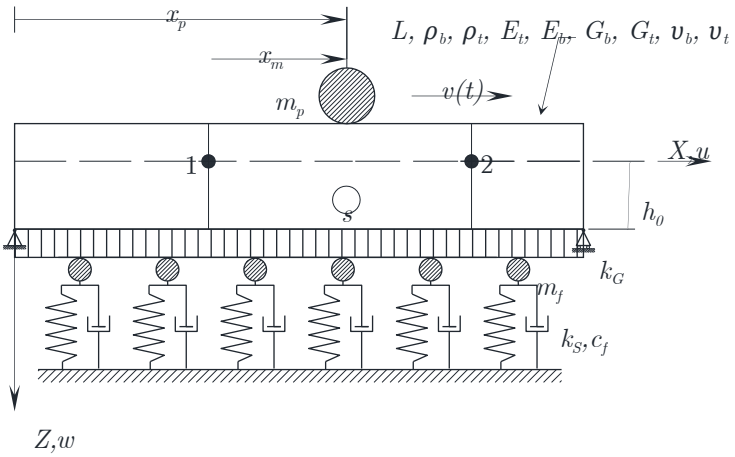

Figure 1. Illustration of the FGM beam, moving mass and the four-parameter foundation.

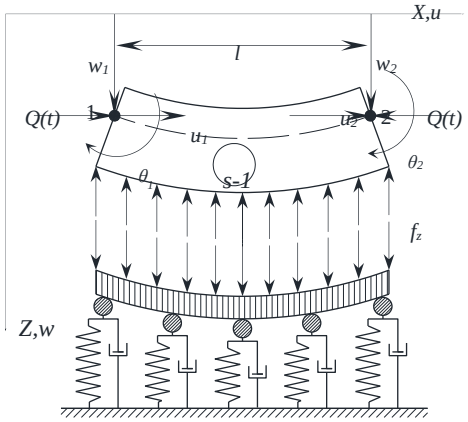

Figure 2. The deformed element (s-1) with the axial force Q(t) applied by an accelerating mass on the element s and the foundation.

In Figure 2, the two-node finite element and the four-parameter foundation are seen from the element contacted by the mass. Here, the finite element is influenced by the Q(t) compressive force resulting from the acceleration of the mass. Adhesive bonding of the foundation with the beam is excellent and the mass of the foundation is in motion together with the beam and the damping cannot be neglected.

Static bonding force between the FGM beam and base are written as

$$f_z = k_{Sz} w(x,t) - k_{Gz} \frac{\partial^2 w(x,t)}{\partial x^2}$$
$$f_x = k_{Sx} u(x,t) - k_{Gx} \frac{\partial^2 u(x,t)}{\partial x^2} \quad (1)$$

In transverse and axial directions, $k_{Sz,x}$ and $k_{Gz,x}$ are the moduli of the subbase respectively.

Displacements in the beam according to TBT are:

$$W(x,z,t) = w(x,t),$$
$$U(x,z,t) = u(x,t) - z\theta(x,t). \quad (2)$$

Where $w(x,t)$, $u(x,t)$,and $\theta(x,t)$ are the transverse and axial displacements, and cross section rotation in the plane at h_0. The constitutive equations of the strains and stresses are:

$$\varepsilon_{xx} = \frac{\partial u}{\partial x} - z\frac{\partial \theta}{\partial x}, \quad \gamma_{xz} = \frac{\partial \omega}{\partial x} - \theta$$
$$\sigma_{xx} = E(z)\varepsilon_{xx}, \quad \tau_{xz} = \kappa G(z)\gamma_{xz} \quad (3)$$

Where κ is the share factor, G(z) and E(z) are the actual share and elasticity module. To describe the actual properties of FGM material two approaches are used in the literature. The exponential law, used in fracture studies of FGMs ([67],[59]) is defined as

$$P(z) = P_t \exp(-\delta(1 - 2z/h)), \quad \delta = 0.5\log(P_t / P_b) \quad (4)$$

The power-law, having all expected features and given by [61], is reported as

$$P(z) = P_b + (P_t - P_b)V_t(z)$$
$$V_t(z) = \left(\frac{z}{h} + \frac{1}{2}\right)^n, V_b = 1 - V_t \quad (5)$$

Where *n* is the exponent, and it represents the mixture rates. *P*(*z*) means (G; ν; E) a specific material property. P_b and P_t, respectively, are the values of the properties at the bottommost and topmost surfaces. Considering foundation and TBT, for the beam element in Fig 2 the strain energy can be written as

$$S = \frac{1}{2}\int_0^l \begin{bmatrix} B_{11}u'^2 - 2B_{12}u'\theta' + B_{22}\theta'^2 + \kappa B_{33}(w' - \theta)^2 \\ + k_{Sx}u^2 + k_{Gx}u'^2 + k_{Sz}w^2 + k_{Sz}w'^2 \end{bmatrix} dx \quad (6)$$

Where $u' = \partial u / \partial x$, $w' = \partial w / \partial x$, $\theta' = \partial \theta / \partial x$, and the rigidities B_{11},B_{12} ,B_{22} and B_{33} are defined as

$$B_{11}, B_{12}, B_{22} = \int_A (1, z, z^2)E(z)dA, \quad B_{33} = \int_A G(z)dA \quad (7)$$

For the beam element itself, the kinetic energy is

$$T = \frac{1}{2}\int_0^l \left[I_{11}(\dot{u}^2 + \dot{w}^2) + I_{22}\dot{\theta}^2 - 2I_{12}\dot{u}\dot{\theta} \right] dx \tag{8}$$

where

$$(I_{11}, I_{12}, I_{22}) = \int_A \rho(z)(1, z, z^2) dA \tag{9}$$

For the beam element with the length *l*, the kinetic energy T_f and the Rayleigh's energy dissipation function *R* of the foundation are

$$T_f = \frac{1}{2} m_f \int_0^l \left(\frac{\partial w}{\partial t} + \frac{\partial u}{\partial t} \right)^2 dx, R = \frac{1}{2} c_f \int_0^l \left(\frac{\partial w}{\partial t} + \frac{\partial u}{\partial t} \right)^2 dx \tag{10}$$

where m_f and c_f are the unit mass and damping of the base and they are assumed to be the same for the transverse and axial movements of the beam. While the mass is moving on the deflected beam, the kinetic energy T_m of it:

$$T_m = \frac{1}{2} m_p \left(v^2 + \left(\frac{\partial w}{\partial t} + v \frac{\partial w}{\partial x} \right)^2 \right)_{x=x_p} \tag{11}$$

Due to the dead load and the acceleration of the mass on the beam, the contact forces in z and x directions are [37]:

1. $$f_{cz}(x,t) = m_p g - m_p \left(\frac{\partial^2 w}{\partial t^2} + 2v \frac{\partial^2 w}{\partial x \partial dt} + v^2 \frac{\partial^2 w}{\partial x^2} + a \frac{\partial w}{\partial x} \right) \delta(x - x_p)$$
2. $$f_{cx}(x,t) \approx m_p a - m_p \left(\frac{\partial^2 u}{\partial t^2} \right) \delta(x - x_p) \tag{12}$$

Where $x_p(t)$, the mass location, is defined with:

3. $$x_p(t) = x_0 + v_0 t + 0.5at^2,\ v = \left. \mathrm{d}x / \mathrm{d}t \right|_{x=x_p}; a = \left. \mathrm{d}^2 x / \mathrm{d}t^2 \right|_{x=x_p}$$ 4. (13)

Due to the acceleration of the mass and consecutively the axial force $Q=m_p a$, the work W^e done on the element is written as

$$W^e = -Q(t) \int_0^l \left(\frac{\partial w}{\partial x} + \frac{\partial u}{\partial x} \right)^2 dx \tag{14}$$

In this study the force $m_p a$ is symmetrically applied at the neutral axis and the moment of it neglected. In heavy vehicle application of moving load [48], for the cases of acceleration and deceleration the moment loadings should be included.

Considering the contact forces between the beam and mass and, the potential energy is

$$V = f_{cz} w(x,t) \delta(x - x_p(t)) + f_{cx} u(x,t) \delta(x - x_p(t)) \tag{15}$$

When the potential and kinetic energy and mass interaction forces are used with the Hamilton principle, in terms of *u*, *w* and *Θ* the motion equation of the whole system is derived as follows:

$$\begin{aligned}
&\delta \mathrm{u}: I_{11}\ddot{u} - I_{12}\ddot{\theta} - B_{11}u'' + B_{12}\theta'' + Qu' + (m_p\ddot{u} - Q)_{x=x_p} = 0\\
&\delta w: I_{11}\ddot{w} - \kappa B_{33}(w'' - \theta') - Qw'\\
&+(m_p\ddot{w} + 2m_p v\dot{w}' + m_p v^2 w'' + m_p a w' - m_p g)_{x=x_p} = 0\\
&\delta\theta: I_{22}\ddot{\theta} - I_{12}\ddot{u} + B_{12}u'' - B_{22}\theta'' - \kappa B_{33}(w' - \theta) = 0,
\end{aligned} \tag{16}$$

and the force boundary conditions

$$B_{11}u' - B_{12}\theta' = N^x;\quad \kappa B_{33}(w' - \theta) = Q^x;\quad B_{22}\theta' - B_{12}u' = M^x;\quad at\ x = 0\ and\ x = L. \tag{17}$$

where Q^x, M^x and N^x, are force resultants at the beam ends. The boundary conditions are :

$$u(x = 0,\ t) = 0\ ,\ w(x,\ t) = 0\ at\ x = 0\ and\ x = L \tag{18}$$

Where $m_p\ddot{w} + 2m_p v\dot{w}' + m_p v^2 w'' + m_p a w'$ and $m_p\ddot{u}$ are the components of the mass interaction forces. The analytical solution of the equation of motion in (16) is quite complex, but the equation can be modelled and solved using FE representations of all parts of the equation as indicated in the following sections. Firstly, for this purpose, FE shape functions are obtained by using the following static part of equation (16) for the FGM beam itself.

$$\begin{aligned}
&B_{11}u'' - B_{12}\theta'' = 0\\
&\kappa B_{33}(w'' - \theta') = 0\\
&B_{12}u'' - B_{22}\theta'' - \kappa B_{33}(w' - \theta) = 0.
\end{aligned} \tag{19}$$

When the partial differential equation in Eq. (19) is solved the following polynomials for the DOFs are obtained.

$$\begin{aligned}
&u = e_1 + e_2 x + e_3 x^2\\
&w = e_4 + e_5 x + e_6 x^2 + e_7 x^3\\
&\theta = e_8 + e_9 x + e_{10} x^2
\end{aligned} \tag{20}$$

The following derivations of polynomials are introduced into Eq. (19) and the four of the unknowns in Eq. (21) are eliminated. The left 6 unknowns are defined using the end conditions of the beam element, at x=0, and at x=*l*.

$$\begin{aligned}
&u'' = 2e_3\\
&w' = e_5 + 2e_6 x + 3e_7 x^2\\
&w'' = 2e_6 + 6e_7 x\\
&\theta' = e_9 + 2e_{10} x\\
&\theta'' = 2e_{10}
\end{aligned} \tag{21}$$

Then, the followings are derived for the inner displacements of the element [64,65]

$$\begin{aligned}
&u = \Psi_u \mathbf{d},\quad w = \Psi_w \mathbf{d},\quad \theta = \Psi_\theta \mathbf{d},\\
&\mathbf{d} = \begin{bmatrix} u_1 & w_1 & \theta_1 & u_2 & w_2 & \theta_2 \end{bmatrix}^T
\end{aligned} \tag{22}$$

where $\mathbf{d}$ is the displacement vector, and $\Psi_u, \Psi_w, \Psi_\theta$ (given in Appendix (A.2-A.4)) shape functions for the nodal displacements. After the interaction terms of the mass and Eq. (16) are evaluated with the interpolation functions of Eq. (22), the following total strain energy of beam and foundation can be expressed as

$$\begin{aligned} S &= \frac{1}{2}\sum_{i}^{r} \mathbf{d}^{\mathbf{T}}\mathbf{k}\mathbf{d} \\ S &= \frac{1}{2}\sum_{i}^{r} \mathbf{d}^{\mathbf{T}} \begin{pmatrix} \mathbf{k}_{uu} + \mathbf{k}_{u\theta} + \mathbf{k}_{\theta\theta} + \mathbf{k}_{\gamma\gamma} + \mathbf{k}_{f1z} + \mathbf{k}_{f2z} \\ + \mathbf{k}_{f1x} + \mathbf{k}_{f2x} + \mathbf{k}_{m}\big|_{i=s} + \mathbf{k}_{G}\big|_{i=1\to s} \end{pmatrix} \mathbf{d} \end{aligned} \tag{23}$$

where, $\mathbf{k}$ is stiffness matrix of the element, which consisting of the axial $\mathbf{k}_{uu}$, coupling $\mathbf{k}_{u\theta}$, bending $\mathbf{k}_{\theta\theta}$, shear $\mathbf{k}_{\gamma\gamma}$ matrices. And $\mathbf{k}_{m}\big|_{i=s}$ is matrix due to centripetal interaction force due to moving mass, and $\mathbf{k}_{G}\big|_{i=1\to s}$ is the geometric stiffness matrix. $\mathbf{k}_{f1z}$, $\mathbf{k}_{f2z}$ and $\mathbf{k}_{f1x}$, $\mathbf{k}_{f2x}$ are respectively represents the foundation stiffnesses in z and x directions. The derivations of the matrices are as follows:

$$\begin{aligned} &\mathbf{k}_{uu} = \int_0^l \Psi'_u{}^T B_{11} \Psi'_u dx, \quad \mathbf{k}_{u\theta} = \int_0^l \Psi'_u{}^T B_{12} \Psi'_\theta dx, \\ &\mathbf{k}_{\theta\theta} = \int_0^l \Psi'_\theta{}^T B_{22} \Psi'_\theta dx, \quad \mathbf{k}_{\gamma\gamma} = \int_0^l (\Psi'_w - \Psi_\theta)^T \kappa B_{33} (\Psi'_w - \Psi_\theta) dx, \\ &\mathbf{k}_{\mathbf{G}} = \mp m_p a \int_0^l \Psi'_w{}^T \Psi'_w dx \\ &\mathbf{k}_{f1z} = \int_0^l \Psi_w{}^T k_{Sz} \Psi_w dx; \\ &\mathbf{k}_{f1x} = \int_0^l \Psi_u{}^T k_{Sx} \Psi_u dx, \Psi_{i,j} (i,j = 1,4) \\ &\mathbf{k}_{f2z} = \int_0^l \Psi'_w{}^T k_{Gz} \Psi'_w dx; \\ &\mathbf{k}_{f2x} = \int_0^l \Psi'_u{}^T k_{Gx} \Psi'_u dx, \Psi_{i,j} (i,j = 1,4) \\ &\mathbf{k}_{m}\big|_{i=s} = [k]_{6x6}, k_{i,j} = m_p (v^2 \Psi_{wi} \Psi''_{wj} + a \Psi_{wi} \Psi'_{wj}), (i,j = 2,3,5,6), \\ &k_{i,j} = 0, (i,j = 1,4) \end{aligned} \tag{24}$$

The kinetic energies of the FGM beam (8), the foundation (10) and the moving mass (11) can be combined as follows:

$$\begin{aligned} T &= \frac{1}{2}\sum_{i}^{r} \dot{\mathbf{d}}^{\mathbf{T}} \mathbf{m} \dot{\mathbf{d}} \\ &= \frac{1}{2}\sum_{i=1}^{r} \dot{\mathbf{d}}^{\mathbf{T}} \left(\mathbf{m}_f + \mathbf{m}_{m}\big|_{i=s} + \mathbf{m}_{\theta\theta} + \mathbf{m}_{ww} + \mathbf{m}_{uu} + \mathbf{m}_{u\theta} \right) \dot{\mathbf{d}} \end{aligned} \tag{25}$$

with $\mathbf{m}_f$ is the foundation mass matrix, and $\mathbf{m}_{m}\big|_{i=s}$ is the matrix of the moving mass interaction, while $\mathbf{m}_{\theta\theta}$, $\mathbf{m}_{ww}$, $\mathbf{m}_{uu}$, $\mathbf{m}_{u\theta}$,are, respectively, mass matrices for displacement DOFs of the FGM beam as seen below:

$$\mathbf{m}_{uu} = \int_0^l {\Psi_u}^T I_{11} \Psi_u dx, \quad \mathbf{m}_{ww} = \int_0^l {\Psi_w}^T I_{11} \Psi_w dx,$$
$$\mathbf{m}_{u\theta} = -\int_0^l I_{12}({\Psi_u}^T \Psi_\theta + {\Psi_\theta}^T \Psi_u) dx, \quad \mathbf{m}_{\theta\theta} = \int_0^l {\Psi_\theta}^T I_{22} \Psi_\theta dx, \tag{26}$$
$$\mathbf{m}_f = \int_0^l {\Psi_w}^T m_f \Psi_w dx$$
$$\mathbf{m}_m\Big|_{i=s} = [m]_{6x6}, m_{i,j} = m_p(\Psi_{wi}\Psi_{wj}), (i,j=2,3,5,6), m_{i,j} = 0, (i,j=1,4)$$

Mass interaction matrices, $\mathbf{k}_m\Big|_{i=s}$ and $\mathbf{m}_m\Big|_{i=s}$ are given in Appendix A.5-A.8

When the Rayleigh's dissipation function in (11) due to viscous damping of the foundation and the Coriolis force $2m_p v\dot{w}'$ of the interaction in (16) used with the beam shape functions the following damping matrices are obtained:

$$\mathbf{c}_f = \int_0^l {\Psi_w}^T c_f \Psi_w dx,$$
$$\mathbf{c}_m = [c]_{6x6}, c_{i,j} = 2m_p v(\Psi_{wi}\Psi'_{wj}), (i,j=2,3,5,6), c_{i,j} = 0, (i,j=1,4) \tag{27}$$

The equivalent viscous damping of the beam element of the FGM beam itself can be obtained using the proportional damping rule as given below:

$$\mathbf{c}_b = a_0 \mathbf{m}_b + a_1 \mathbf{k}_b,$$
$$a_0 = \frac{2\omega_i\omega_j(\zeta_i\omega_j - \zeta_j\omega_i)}{{\omega_j}^2 - {\omega_i}^2}, a_1 = \frac{2(\zeta_j\omega_j - \zeta_i\omega_i)}{{\omega_j}^2 - {\omega_i}^2} \tag{28}$$

where $\mathbf{m}_b = \mathbf{m}_{\theta\theta} + \mathbf{m}_{ww} + \mathbf{m}_{uu} + \mathbf{m}_{u\theta}$ and $\mathbf{k}_b = \mathbf{k}_{uu} + \mathbf{k}_{u\theta} + \mathbf{k}_{\theta\theta} + \mathbf{k}_{\gamma\gamma}$ are the property matrices of the beam element, and the terms ζ_i and ζ_j represent the damping ratios for the natural frequencies ω_i and ω_j.

3 Motion equation of the FGM beam-foundation system

For the multy-Dof damped system in Figure1, the motion equation can be described as:

$$\mathbf{M}\ddot{\mathbf{q}} + \mathbf{C}\dot{\mathbf{q}} + \mathbf{K}\mathbf{q} = \mathbf{F}, \tag{29}$$

In the equation given above, **M**, **C** and **K** are the property matrices and they are obtained from the assembly of the property matrices of the elements given in equations (24-28). When creating matrices, the property matrices of all elements except the finite element s are normally created by adding the parameters of the foundation. Depending on the movement of the mass of the matrices of the element s where the mass is momentarily located are modified by the addition of the matrices of $\mathbf{m}_m$, $\mathbf{k}_m$ and $\mathbf{c}_m$ resulting from mass interaction. For the elements in which the mass is not in contact, the damping matrix **C** is the sum of the $\mathbf{c}_f$ and $\mathbf{c}_b$ matrices. The general external force vector **F** consists of zero coefficients except the force coefficients of the element s. Thus, the force vector is:

$$\mathbf{F} = \begin{bmatrix} 0 & \dots & \mathbf{f}_m & \dots & 0 \end{bmatrix}^T \tag{30}$$

The coefficients of nodal force vector $\mathbf{f}_m$ (6x1) of the beam element s are derived using the procedure given in Appendix (A.8)

4 Numerical examples and findings

4.1 *Validation*

In order to confirm, the fundamental frequencies obtained by applying this method to an FGM beam studied in the literature [49,66] are given in Table 1. Where, the fundamental frequency parameter (32) of the FGM beam is obtained using TBT (FSDBT2 in [66] for Alumina and Aluminium with the following material properties:

Alumina (%99.5) : υ= 0.23; ρ = 3800 kg/m^3; E= 380 GPa
Aluminium : υ =0.23; ρ = 2700 kg/m^3; E =70 GPa

The undamped free vibration solution of Eq. (29) results:

$$(\mathbf{K} - w_n^2\mathbf{M})\mathbf{q} = 0, \tag{31}$$

Without the effect of the foundation, where k_S=k_G=m_f=c_f=0, the frequencies of the FGM beam itself are determined using the non-trivial solution, where, $\mathbf{K} - w_n^2\mathbf{M}$ =0. Considering the effective material properties of the FGM beam, the frequency parameter λ_1 of the first mode is defined by using

$$\lambda_1 = w_1 L^2 \frac{\sqrt{\int_{-h/2}^{h/2} \rho(z)dz}}{\sqrt{h^2 \int_{-h/2}^{h/2} E(z)dz}} \tag{32}$$

In Table 1, the results of the presented method and the one in Ref.[49] are quite close to each other and the harmony between them is satisfactory.

Table 1
The first frequency parameter (λ_1) for the FGM beam with Al -Al2O3

n		λ_1		
	Refs.	*L/h*=10	*L/h*=30	*L/h*=100
0	From [49]	2.7970	2.8430	2.8480
	From [66]	2.8026	2.8438	2.8486
	Present	2.8027	2.8458	2.8488
0.3	From [49]	2.6950	2.7370	2.7420
	From [66]	2.6992	2.7368	2.7412
	Present	2.6953	2.7361	2.7421

Table 3 shows the comparison of this study and others [50,51]41,42] for a FGM beam of 99.9% pure alumina and stainless steel (SUS 304) and its characteristics given in Table 2 for comparison with the moving loads studies in literature. The results of [50] and this study are in very good agreement .

Table 2
Constituents of the FGM

Properties	Unit	SUS304	Al2O3, %99.9
υ	-	0.3177	0.3
ρ	kg/m^3	8166	3960
E	GPa	210	390

Table 3
The maximum mid-span responses to a load moving at constant velocities, for FGM beam with $k_S=k_G=m_f=c_f=0$.

Source	SUS304 (132 m/s)	n=0.2 (222 m/s)	n=0.5 (198 m/s)	n=1 (179 m/s)	n=2 (164 m/s)	n=5 (164 m/s)	Al2O3 (252m/s)
[50]	1.7324	1.0344	1.1444	1.2503	1.3376	-	0.9328
[51]	1.7301	1.0333	1.1429	1.2486	1.3359	-	0.9317
Present	1.7316	1.0336	1.1435	1.2690	1.3365	1.6314	0.9326

In order to prove the precision of the new formulation with the effect of the foundation, the results of this study were compared with the results in the literature. The fundamental frequencies given in Table 4 are compared with the reported ones in [35], based on Euler-Bernoulli's theorem for a beam on a foundation model with $\boldsymbol{k_S}$ and $\boldsymbol{k_G}$ and without the effects of damping and mass density, where the foundation parameters are defined in terms of the dimensionless parameters given in equation (34).

$$K_1 = \frac{k_S L^4}{EI} \quad , K_2 = \frac{k_G L^2}{\pi^2 EI}, \lambda_1 = \omega L^2 \ \left(\rho A / EI\right)^{1/2} \tag{34}$$

Table 4. The Fundamental frequency parameter λ_1 of the beam for different foundations.

		K_1					
	K_2	0	10	10^2	10^3	10^4	10^5
Present study	1	13.9577	14.3115	17.1703	34.5661	100.9694	316.5356
[35]	1	13.9577	14.3115	17.1703	34.5661	100.9694	316.5356

4.2 Case study

To examine the effect of the parameters of the base, a new FGM beam consisting of aluminium and zirconium oxide was studied. Where L = 24 m, h = 0.8 m, b = 0.5 m. Table 5 shows the material properties of the constituents that are Aluminium (Al) at -h/2 and full Zirconia (ZnO_2) at h/2. A 100 kN moving load, which corresponds to 1019.7 kg of moving mass, was moved over the FGM beam supported by four-parameter bases, with the increments of 1 m / s between 0-250 m / s. The step number in the Newmark integration was set to 250 and the FGM beam was divided into 12 finite elements. The analyses were carried out separately by taking into consideration the moving mass and moving load cases and the results were presented in Figs 3-8 for power law index n of the FGM beam and different mass, damping and stiffness modules of the foundations. In all the results given in all the Figs, the normalization of the displacements was made according to the static collapse of the midpoint w_0 of the beam consisting of full aluminium for n = infinite. Here $w_0 = mgL^3 / 48EI$. In the case where the parameters of the foundation are equal to zero, the dynamic amplification factors (DAFs $= w_{max}\,(L/2, t) / w_0$) of different mixtures of the FGM beam are given in Figure 3 according to the mass velocity and index n. the graphs on the left and right show the results of the moving load and mass cases respectively. Also, for the different foundation parameters, the maximum values of the DAFs and mass speeds are given in Table 6. In the cases of zero damping c_f = 0, and without accounting of the mass effect m_f = 0, Figure 4 depicts the effects of the parameters of the bases on the response. Here, the shear foundation parameter K_2 is fixed to 1, and the non-dimensionless parameters of the spring foundations are accepted at four different values, K_1 = $10,10^2,10^3,10^4$. Graphs show a significant decrease in displacements due to the increase in stiffness of the

spring foundation. Additionally, it can be directly realised that the stiffnesses of the base also accordingly changes the vibration form of the FGM beam. This is already an expected situation, in which the size of the additional foundation stiffnesses alters the vibration characteristic of the whole system. Here, for FGM beams the term D_{22} given in Eq. (7) is used instead of *EI* of the homogeneous materials. Table 7 shows the calculated geometric and material properties of the considered FGM beam where, the effective bending stiffness in the first column, the second moment of inertia of the cross section in the second one, and the effective elasticity modulus in third one, and the rest of the columns are for the beam mass, the mass of the load and the mass ratio ε (moving mass / beam mass), respectively. Figure 5 depicts the effect of the foundation mass at different ratios by taking $K_1 = 10$, $K_2 = 1$ and damping $c_f = 0$. The unit length mass of the full Aluminium beam with the chosen dimensions is 2280 kg. In the analyses the masses of the foundation are 1140, 2280 and 4560 kg/m when the mass ratios, that is the unit mass of the foundation / unit mass of the beam m_f / m_b, are 0.5, 1 and 2. It should be known that the foundation mass may vary according to type of the application. For example, in applications such as soil, ballast, it is more accurate to accept the mass of the foundation portion that is thought to move with the FGM beam. Otherwise, for a specially designed suspension system the mass m_f is obtained from the design dimensions. Fig 6 shows the effect of the foundation damping on the dynamics of the FG beam for $K_1 = 10$, $K_2 = 1$, $m_f / m_b = 0.5$ and different viscous damping coefficients of $c_f = 10^3$, 5.10^3 and 10.10^3 Ns/m. In addition, the effects of the viscous damping and mass are summarized in Tables 8 and 9, respectively. The tables give valuable information about the dynamic response of the beam supported by different foundations. In the tables, vibration DAFs and their corresponding mass velocities are given for the moving mass and moving load cases. Generally, in the moving load case, the increase in the foundation mass and damping do not affect the amplitudes of the DAFs too much, but they affect greatly the corresponding velocities of the DAFs. Whereas in the moving mass cases, both the DAFs and the respective travel velocities vary greatly depending on mass and damping. The main reason of these behaviours is that the actual frequency of the whole system is varying depending of the mass involvement and the foundation parameters. The well-known velocity parameter, the exciting frequency of the load / frequency of the beam, also changes depending on the frequency variation of the system. The exciting frequency of the mass is $\omega = \pi v / L$ as reported by [68] and the velocity parameter is defined by ω / ω_1 for the fundamental frequency ω_1. When the speed parameter is 1, the maximum displacement happens. In the case of relatively small damping coefficients, in Table 9, the effect of the damping is very little when compared to the other parameters, K1, K2 and *mf / mb*. The effects of the low damping coefficients are less than 1/10000 for DAFs.

Table 5
Properties of ingredients of the FGM

Properties	Aluminium (Al)	Zirconia (ZnO_2)	Unit
E	70	200	GPa
ρ	2702	5700	kg/m^3
υ	0.23	0.3	-

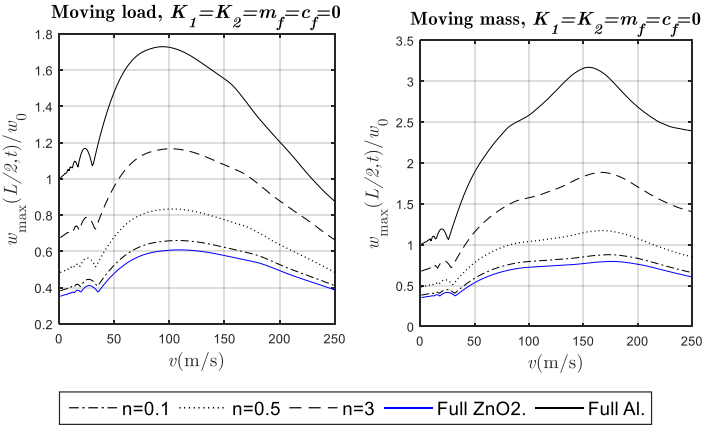

Figure3. Maximum response of the FG beam versus load velocity for different material components, considering the moving mass and load cases.

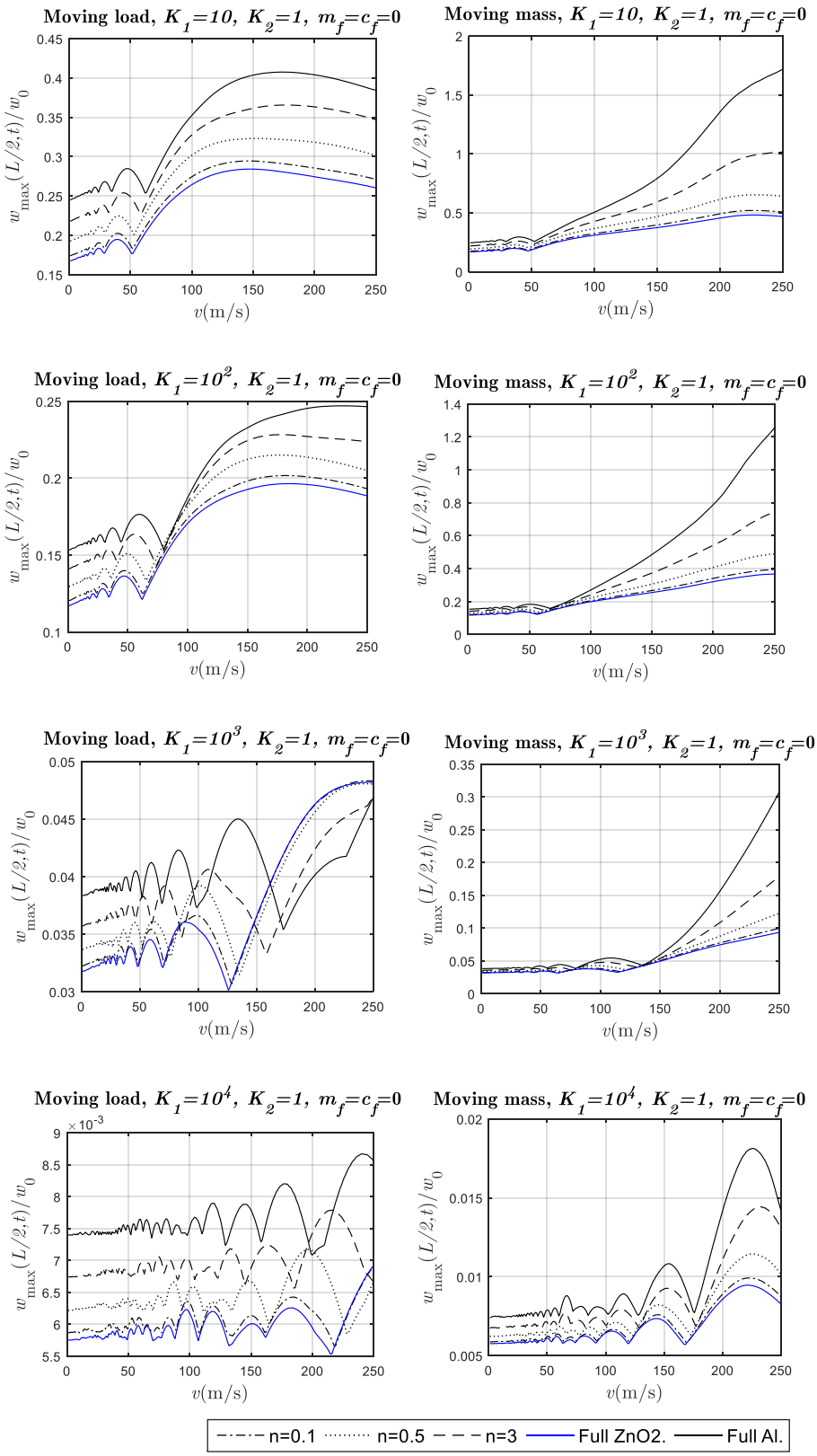

Figure 4 The effect of the spring foundation for different $K_1=10^1$, 10^2, 10^3, 10^4 , and constant $K_2=1$,and $m_f=c_f=0$, left moving load, right moving mass.

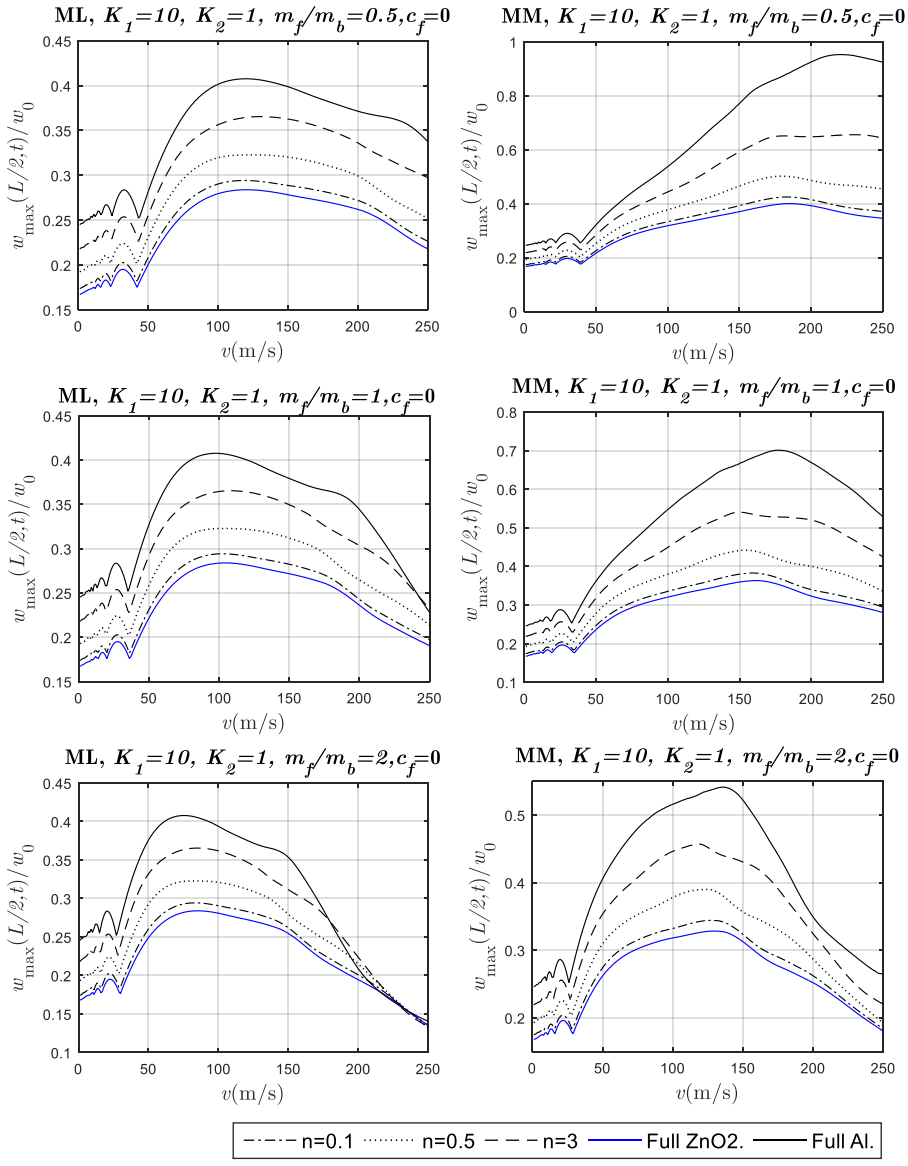

Figure 5. The effect of mass ratio of the foundation for K_1=10, K_2=1and c_f=0. ML: Moving Load, MM: Moving Mass

Table 6
Velocity dependent DAFs of FGM beams of different *n*

	$K_1=0, K_2=0, m_f=0, c_f=0$				$K_1=10\ K_2=1, m_f=0, c_f=0$			
	ML (Moving load)		MM (Moving mass)		ML		MM	
Power-law exponent n	w_{max}/w_0	v (m/s)	w_{max}/w_0	v (m/s)	w_{max}/w_0	v (m/s)	w_{max}/w_0	v (m/s)
0.1	0.660	107	0.878	174	0.295	146	0.519	225
0.5	0.834	103	1.174	167	0.323	152	0.653	228
3	1.166	101	1.885	167	0.366	176	1.015	250
Full ZnO2	0.609	109	0.795	177	0.284	148	0.481	226
Full Al	1.729	94	3.171	155	0.408	173	1.719	250

Table 7
Calculated material and geometric properties of the studied FG beam depending on *n* index.

Power-Law index, *n*	D_{22} (Nm^2)	I (m^4)	E (Pa)	m_b (kg)	m_p (kg)	$\varepsilon=m_p/m_b$
0.1	3.93E+09	0.0209057	1.88E+11	52104	10194	0.195641
0.5	3.11E+09	0.0198756	1.57E+11	45126	10194	0.225894
3	2.23E+09	0.0217227	1.03E+11	33134	10194	0.307651
Full ZnO2	4.27E+09	0.0213333	2.00E+11	54720	10194	0.186288
Full Al	1.50E+09	0.0214117	7.01E+10	25968	10194	0.392549

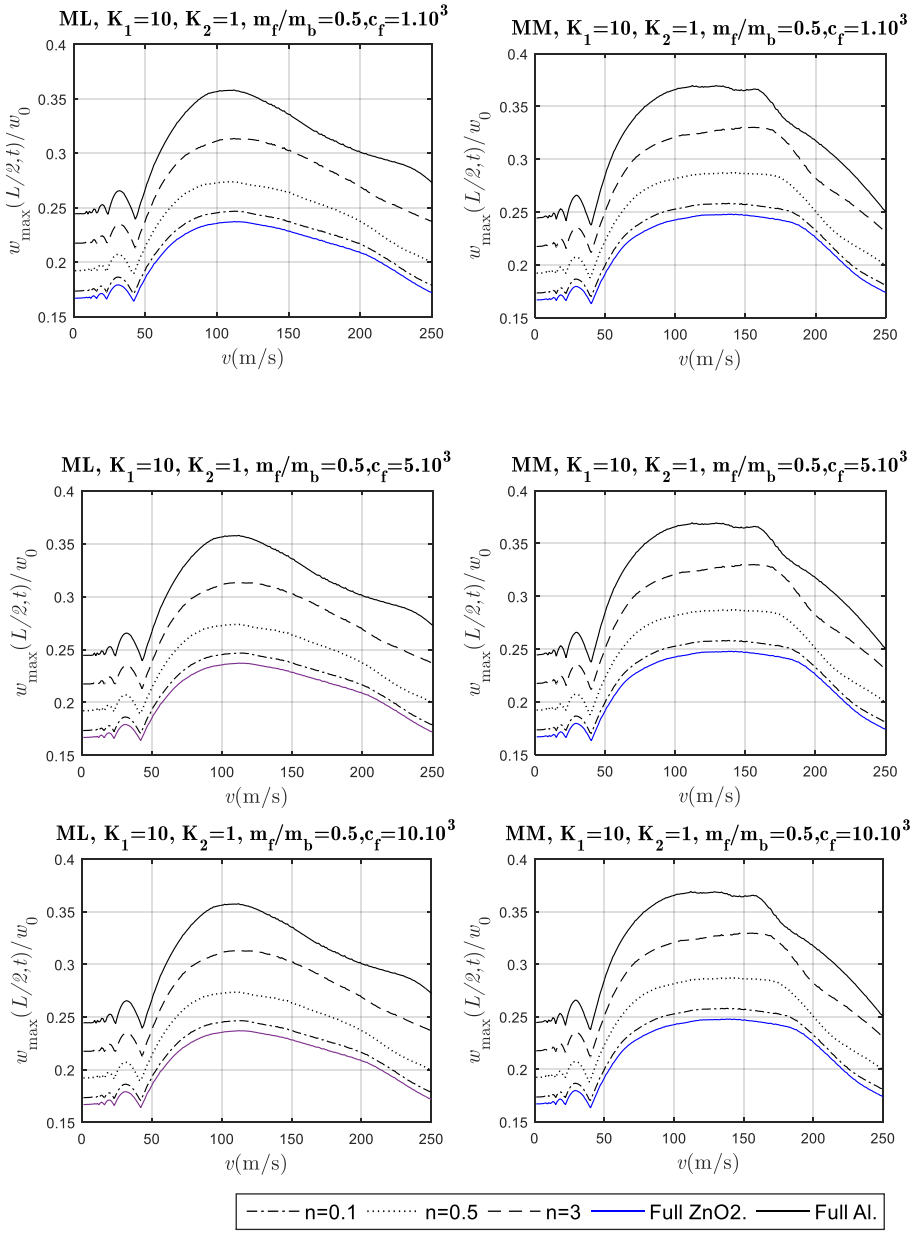

Figure 6. The damping effect of the foundation for different damping parameters c_f= 1.10^3, 5.10^3 and 10.10^3 Nsm^{-1}, for constant K1=10, K2=1, m_f/m_b=0.5. ML: Moving Load, MM: Moving Mass

Table 8
DAFs of the mid-span of the FG beams depending on the *n* and different foundation parameters.

	K_1=10, K_2=1, m_f/m_b=0.5, c_f=0				K_1=10, K_2=1, m_f/m_b=1, c_f=0				K_1=10, K_2=1, m_f/m_b=2, c_f=0			
	ML		MM		ML		MM		ML		MM	
Power-law exponent *n*	w_{max}/w_0	v (m/s)	w_{max}/w_0	v (m/s)	w_{max}/w_0	v (m/s)	w_{max}/w_0	v (m/s)	w_{max}/w_0	v (m/s)	w_{max}/w_0	v (m/s)
0.1	0.29427	119	0.42471	184	0.29428	103	0.38288	159	0.29431	83	0.34412	126
0.5	0.32281	125	0.50179	180	0.32280	106	0.44204	154	0.32282	82	0.38996	125
3	0.36547	130	0.65547	231	0.36547	108	0.54031	150	0.36546	85	0.45717	118
Full ZnO2	0.28391	120	0.40032	185	0.28394	104	0.36325	162	0.28396	85	0.32835	129
Full Al	0.40766	121	0.95240	221	0.40770	98	0.70081	177	0.40780	76	0.54136	136

Table 9
DAFs of the mid-span of the FG beams for *n* and different foundation parameters.

	K_1=10, K_2=1, m_f/m_b=0.5, c_f=10^3				K_1=10, K_2=1, m_f/m_b=0.5, c_f=5.10^3				K_1=10, K_2=1, m_f/m_b=0.5, c_f=10.10^3			
	ML		MM		ML		MM		ML		MM	
Power-law exponent *n*	w_{max}/w_0	v (m/s)	w_{max}/w_0	v (m/s)	w_{max}/w_0	v (m/s)	w_{max}/w_0	v (m/s)	w_{max}/w_0	v (m/s)	w_{max}/w_0	v (m/s)
0.1	0.24692	112	0.25835	138	0.24680	112	0.25820	138	0.24666	112	0.25802	138
0.5	0.27395	112	0.28744	147	0.27381	112	0.28726	147	0.27364	112	0.28703	147
3	0.31372	112	0.33046	151	0.31352	112	0.33014	151	0.31328	112	0.32976	151
Full ZnO2	0.23729	112	0.24810	138	0.23718	112	0.24797	138	0.23705	112	0.24780	138
Full Al	0.35820	112	0.36984	112	0.35790	112	0.36957	112	0.35752	112	0.36922	112

Considering various foundation parameters and mass ratios ε, Figure 7 depicts the frequency variation of the studied beam with the material properties of n = 0.5. The calculated total beam mass is 45126.0 kg, and for the mass ratios of ε=0.1,0.5 and 1 the masses of the moving loads in the analyses are 4512.6, 22563 and 45126 kg respectively. In the analyses, the spring foundation parameters K1 = 0,10,100,1000 and 10000 were changed, keeping the foundation mass and damping at zero, and keeping the shear foundation parameter constant at K2 = 1. Since the load mass is not accounted in the moving load case, the moving mass case is used only in the calculation of the frequency change. As shown in Figure 7, the large mass ratio causes large change in the frequency, and this change also varies with the mass position on the span. The fundamental frequency of the system is increases when the foundation spring stiffness is increased, and the change in relation to the mass location almost preserves the characteristic at low foundation spring stiffnesses. But, in very high foundation spring stiffness parameters, for example, at K1 = 10^3 and 10^4, the bases of the change graphs are flattened. The reason is that in the case of very high foundation spring coefficients, the FGM beam- foundation and mass interaction system is approaching the quasi static loading situation, which is already understandable from the frequency increments of the system.

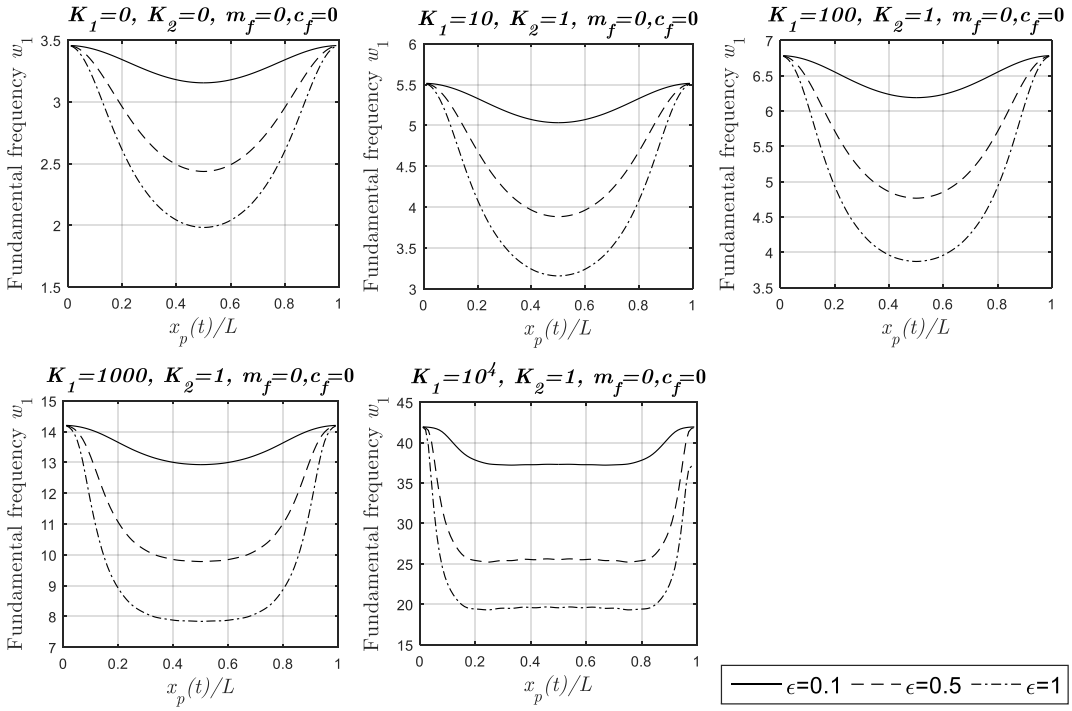

Figure 7. Change of the first natural frequency ω_1 of the FGM beam of n=0.5 and resting on with various foundation stiffness parameters K_1=0, 10 10^2 10^3 10^4 and constant K_2=1 and m_f=c_f=0, depending on the mass ratios of ε=0.1, 0.5 and 1, and the dimensionless mass position $x_p(t)/L$.

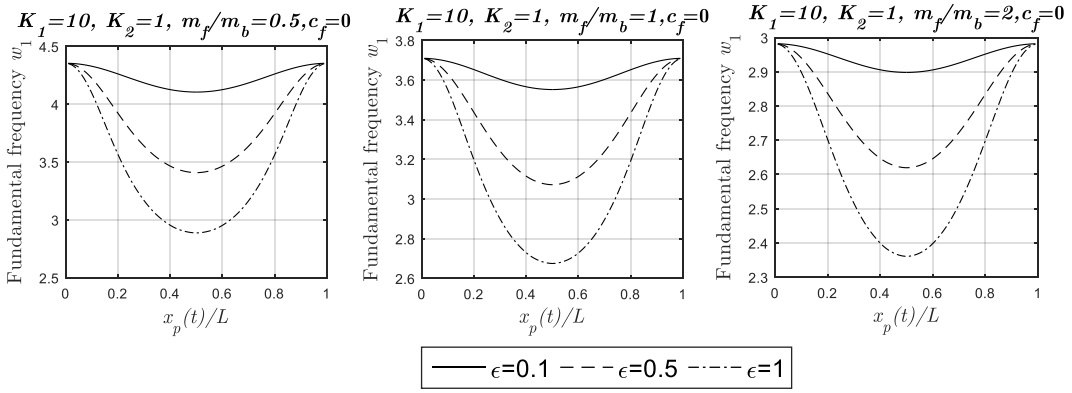

Figure 8. The fundamental frequency variation of the FGM beam of n=0.5 supported by a base with constant dimensionless parameters of K_1=10, K_2=1 and c_f=0, and various m_f/m_b=0.5, 1, 2, depending on the mass ratios of ε=0.1, 0.5 and 1, and the dimensionless mass position $x_p(t)/L$.

Figure 8 shows the alteration of ω_1 of the beam of n=0.5 and on the foundation with the parameters of K_1=10, K_2=1 and c_f=0, and for various m_f/m_b=0.5, 1, 2, depending on the mass ratios of ε=0.1, 0.5 and 1, and the dimensionless position of the mass $x_p(t)/L$. The effect of the mass of the foundation is also considerable and as expected it degreases the fundamental frequency as shown in Figure (8). And the contribution of the mass of the moving load is more effective in relation with the position and ratio ε of the load.

The effect of different mass velocities (v = 20, 40, 60 m / s) on the vibrations of the FGM beam is given in Figure 9 and 10. In the results of Figure 9 all parameters of the foundation are taken as zero, but in the results of Figure 10 the parameters of the foundation are K_2 = 1 constant and K_1=10, 10^2, 10^3, 10^4, and c_f= m_f/m_b=0. For the cases of moving load (ML) and moving mass (MM), the DAF results of different foundation parameters and the mass locations are summarized in Tables 10 and 11

Considering the cases of the ML (left) and MM (right), the results are given in different graphs. In the results, the maximum responses and matching mass locations are dissimilar, and the responses are greater by 125% in the case of the MM. As given in Figure 10, the small foundation stiffnesses have reduced the maximum DAFs have not significantly affected the vibration shape. However, as shown in the figures below, the DAFs have been reduced in the larger stiffnesses of the foundation and the vibration shape have been altered. When the figures in Fig 10 for K1=10^3 and 10^4 are examined closely, the DAFs are considerably small, and the maximums are occurred when the mass is nearly at the middle of the beam, as if the loading of the system is approaching to the quasi static loading case. From the last figure where $K_1=10^4$, the inverse effect of the travelling velocity is nearly eliminated since the responses of different small and high velocities are converged and are very close to each other with a small fluctuation. From this result it is understood that the response of any critical beam-foundation system can be adjusted to satisfy the prescribed design specifications by designing a proper foundation.

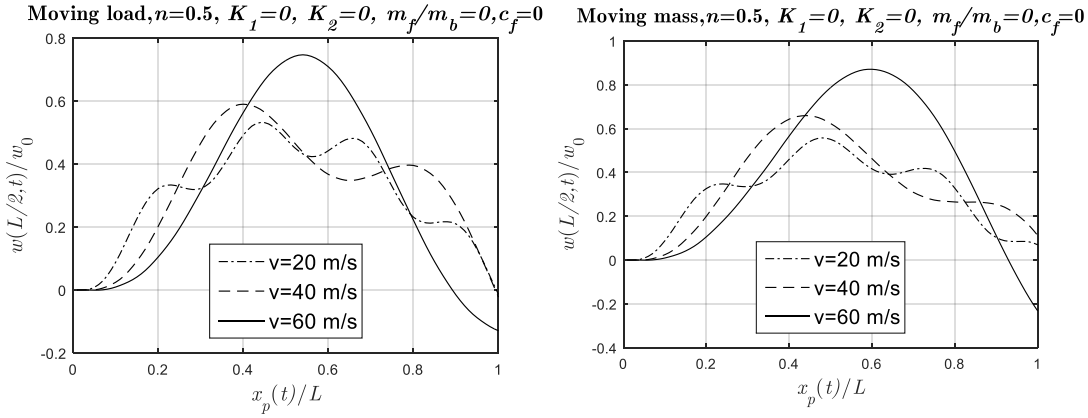

Figure 9. The time histories of midpoint responses for n=0.5, K_1=K_2=m_f=c_f=0 and v=20, 40, 60 m/s,

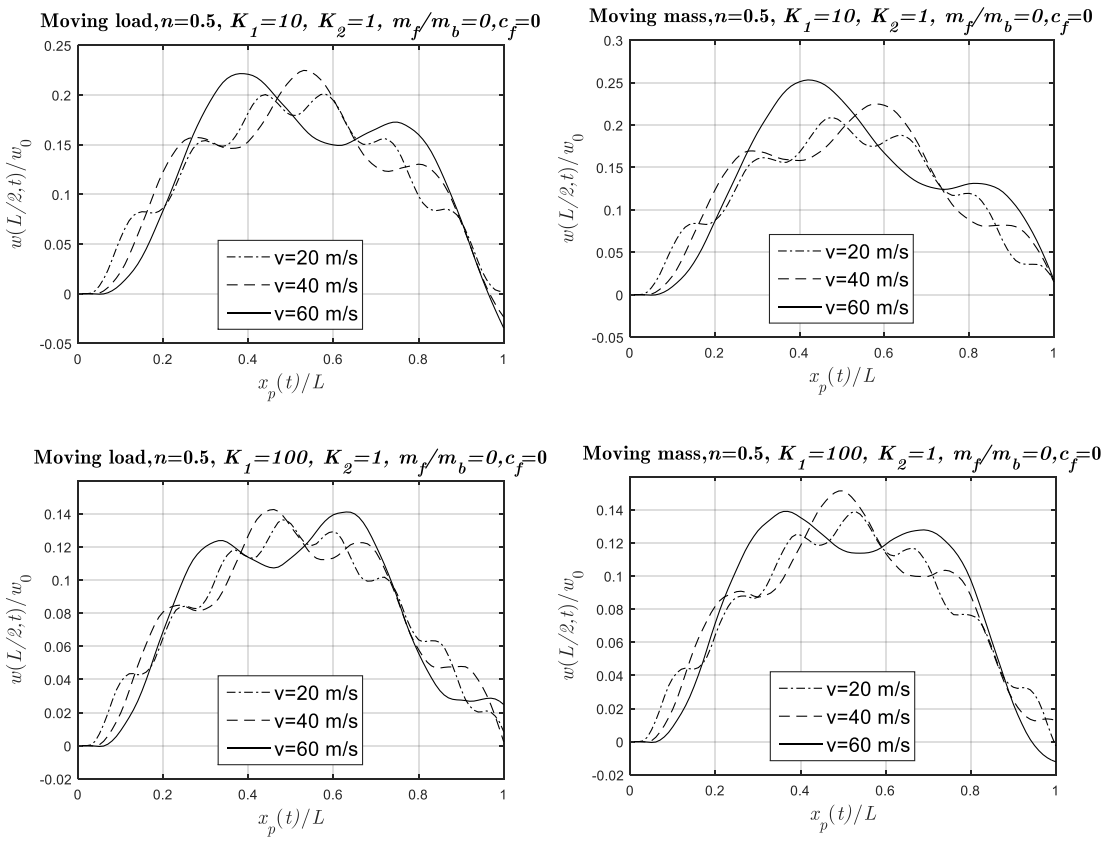

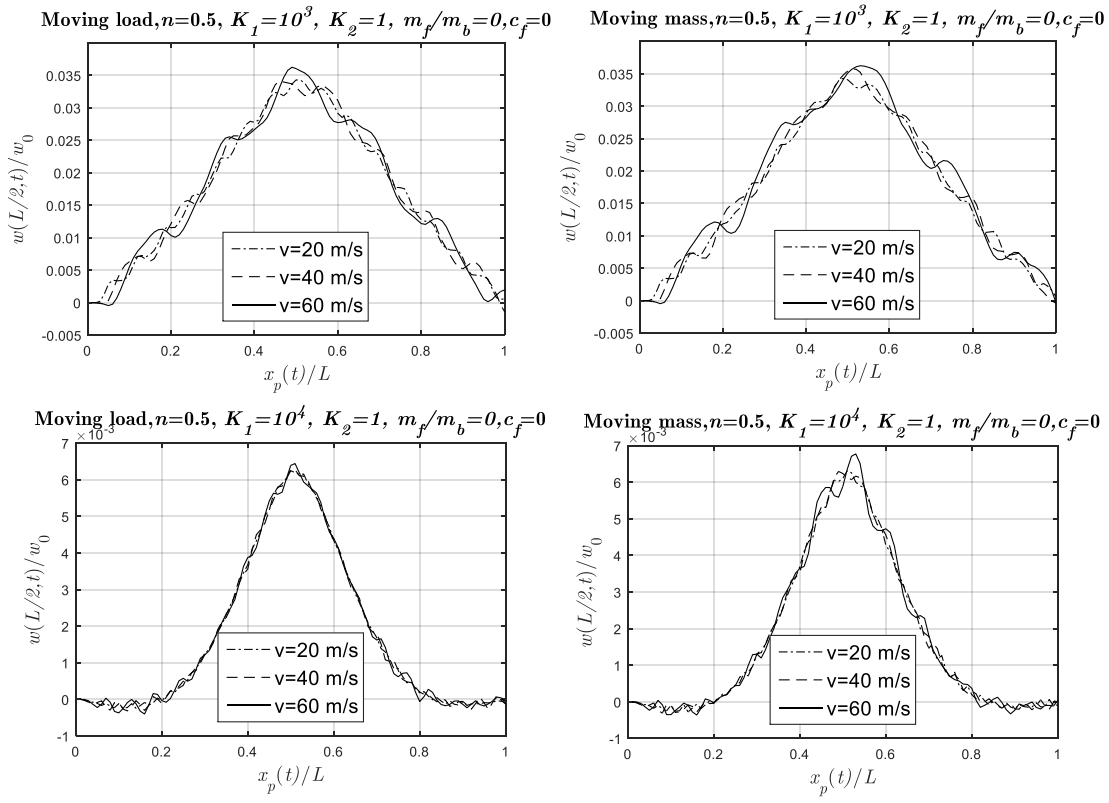

Figure 10. The histories of the midpoint responses of the FGM beam for n=0.5, K_1 =0,10,10^2 10^3 10^4 and constant K_2=1, and m_f=c_f=0, and v=20, 40, 60 m/s.

Table 10
Maximum normalized responses of the mid-span of the FGM beam and the relative place of the mass depending on different foundation parameters and constant n =0.5

	n=0.5, K_1=0, K_2=0, m_f=0, c_f=0				n=0.5, K_1=10, K_2=1, m_f=0, c_f=0				n=0.5, K_1=100, K_2=1, m_f=0, c_f=0			
	ML		MM		ML		MM		ML		MM	
v (m/s)	w/w_0	$x_p(t)/L$	w/w_0	$x_p(t)/L$	w/w_0	$x_p(t)/L$	w/w_0	$x_p(t)/L$	w/w_0	$x_p(t)/L$	w/w_0	$x_p(t)/L$
20	0.532	0.44	0.557	0.48	0.201	0.58	0.208	0.48	0.136	0.48	0.139	0.53
40	0.590	0.4	0.659	0.44	0.225	0.53	0.225	0.58	0.143	0.46	0.151	0.50
60	0.747	0.54	0.871	0.60	0.221	0.38	0.253	0.42	0.141	0.63	0.139	0.37

Table 11
Maximum displacements of the mid-span of the FGM beam and the relative place of the mass depending on different foundation parameters and constant n =0.5

	n=0.5, K_1=10^3, K_2=1, m_f=0, c_f=0				n=0.5, K_1=10^4, K_2=1, m_f=0, c_f=0			
	Moving load		Moving mass		Moving load		Moving mass	
v (m/s)	w/w_0	$x_p(t)/L$	w/w_0	$x_p(t)/L$	w/w_0	$x_p(t)/L$	w/w_0	$x_p(t)/L$
20	0.034	0.50	0.034	0.49	0.006	0.50	0.006	0.51
40	0.034	0.46	0.036	0.52	0.006	0.50	0.006	0.49
60	0.036	0.49	0.036	0.53	0.006	0.51	0.007	0.53

The effects of the foundation mass are plotted in Figure 11 for v = 20, 40 and 60 m/s, and constant stiffness parameter K_1=10, and shear foundation parameter K_2=1. As can be seen from the figures, the mass velocity increase rises the responses. In addition, for the same velocities higher mass of the foundation increases the response of the beam. This is because the additional base mass decreases the frequency ω1 of the whole system and thus increases the speed parameter. The effect of the mass of the

foundation is more effective at higher speeds (v = 60 m / s), as shown in the figure below. From the above results, it is understood that in high speed applications it is necessary to consider the mass of the foundation. Figure 12. Shows the midpoint response of the FGM beam for constant K_1=10, K_2=1, m_f=0, and various travelling velocities of the mass with v=20, 40 and 60 m/s, and various foundation damping coefficients of c_f =5.10^3 and 2.10^5 Nsm^{-1}, and n=0.5. The effect of the viscous damping on the response of beam and foundation system is little when compared to the other parameters of the foundations. Although, the damping coefficient c_f is considerably grate, its effect is remained small in the dynamic interaction when the stiffness parameters of the foundations are high such as K1=10 and K2=1. In such systems damping can be thought for reducing the dynamic amplitudes of the responses when the speed parameter approaches to unity. But it is itself not a significant design parameter when compared the other stiffness parameters of the foundations. As can be seen from Fig 13 the damping is not important in the velocity behaviour of the dynamic response of the whole system. The responses of different velocities are close each other in little and greater damping coefficients of the foundation because it slightly affects the frequency of the entire system.

When an acceleration of the mass is considered for example for a sudden acceleration of the mass from zero to a relatively grater velocity along the span of the beam, Figure 14. depicts the responses of such an acceleration of the mass at a rate of 200 m/s^2, where at the end of the span the velocity reaches to nearly 97 m/s, while Fig 15 depicts the responses for a deceleration of -200 m/s^2. When Figs.14 and 15 shows that the interactions of the mass and the beam-foundation system are very dissimilar in acceleration and deceleration cases. The responses are considerably greater in deceleration case because of the higher velocities of the mass in the interaction is valid in deceleration case. Further, the positions of the mass on the beam when the maximum responses occur are different, for example the relative position of the mass at the deceleration is about 0.4 of the span-length, but at the acceleration it is about 0.7-0.8. In the cases of acceleration / deceleration movements, the results of moving mass and load case are quite different. In the case of acceleration / deceleration movements, the results of moving load and mass assumptions are quite different. In the moving mass case at acceleration the response are 2.5 times higher than the assumption of moving load; and at deceleration, the responses are 5 times higher. The reason for this is that the effects of mass inertia due to high mass velocity and acceleration are high enough to significantly affect the beam dynamics. From this it can be understood that in cases of high-variable-velocity movement of the loads, in the response calculation of the systems the mass inertia should be accounted.

As in other cases, the greater foundation parameters are very effective on the reduction of the magnitude of the responses in the acceleration / deceleration situations. The effects of this acceleration or deceleration and their consideration in engineering calculations will be even more important in today's and future civil engineering applications, as the speed of transport systems is increasing. Also, in civil engineering applications of the moving loads the travelling velocities are examined in terms of the separation phenomena of the beam and mass system. This separation can occur when the sing of the interaction force in Eq. (13) changes, but in this study no separation is allowed, and the continuous contact is maintained in the motion of the load. Due to the nature of application in precision metalworking and rocket launch systems, separation is not created, but separation should be accounted, especially in VBI applications.

In the presence of acceleration and Q (t), axial vibration of the beam is excited, and in such a case, one can analyse the axial vibration with the methods and formulations given in this study using axial force and axial stiffness matrices given in Eqs.13, 16 and 25. To highlight the transverse effect of the moving mass on the FGM beam-foundation system, no result of the axial interaction is given in the analysis results.

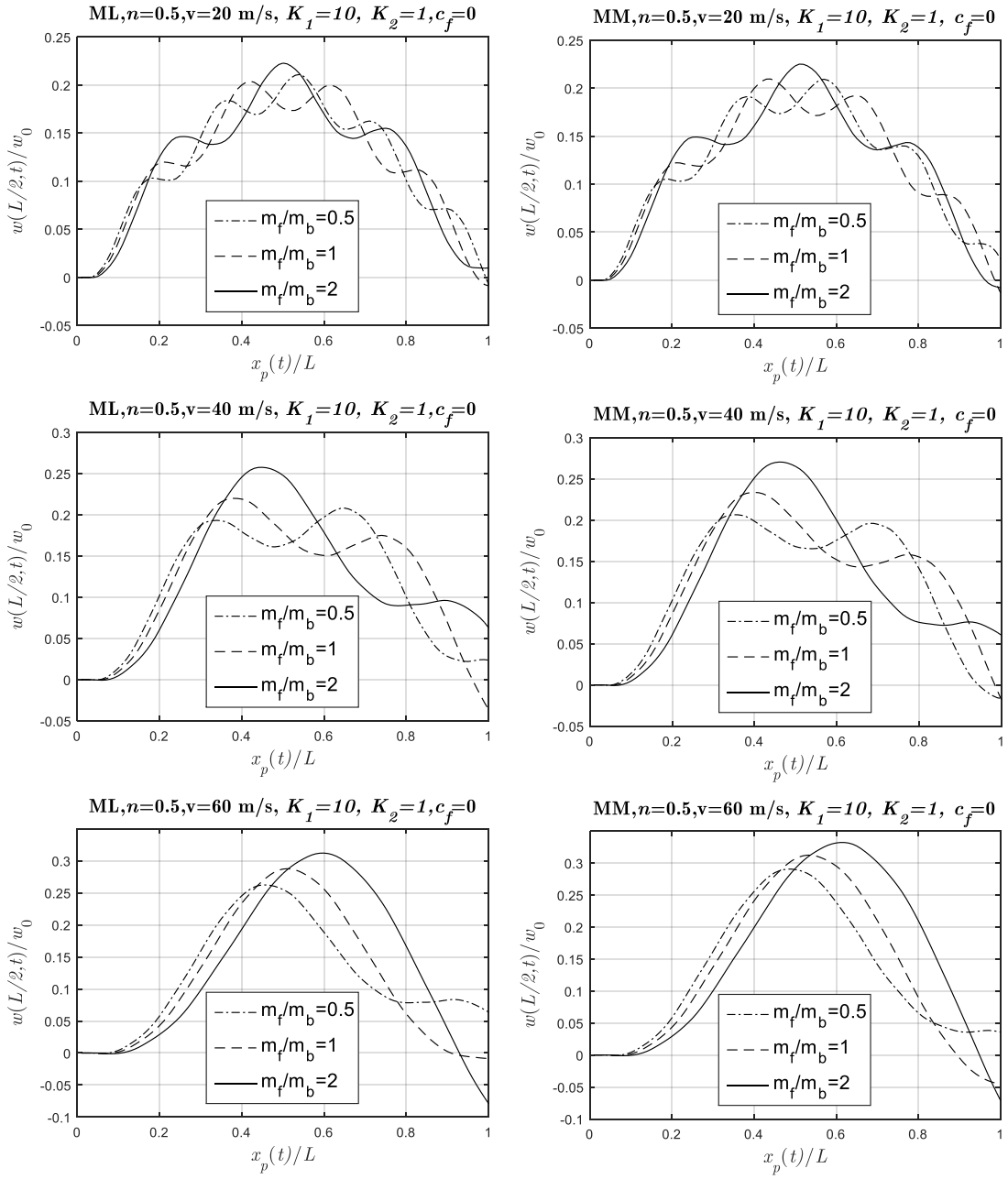

Figure 11. The midpoint response of the FGM beam for constant K_1=10, K_2=1, and various travelling velocities of the mass with v=20, 40 and 60 m/s, and various foundation mass ratios of m_f/m_b=0.5, 1 and 2, and n=0.5. where ML is moving load and MM is moving mass cases.

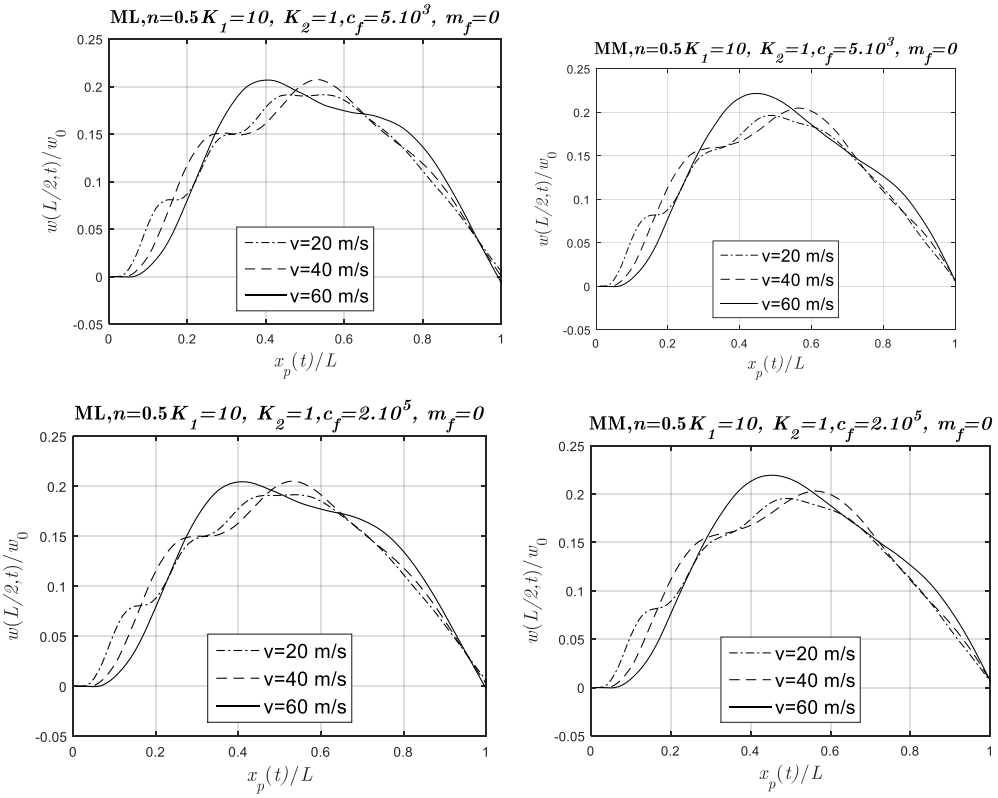

Figure 12. The midpoint response of the FGM beam for constant K_1=10, K_2=1, m_f=0, and various travelling velocities of the mass with v=20, 40 and 60 m/s, and various damping coefficients of c_f =5.10^3 and 2.10^5 Nsm^{-1}, and n=0.5. where ML is moving load and MM is moving mass cases.

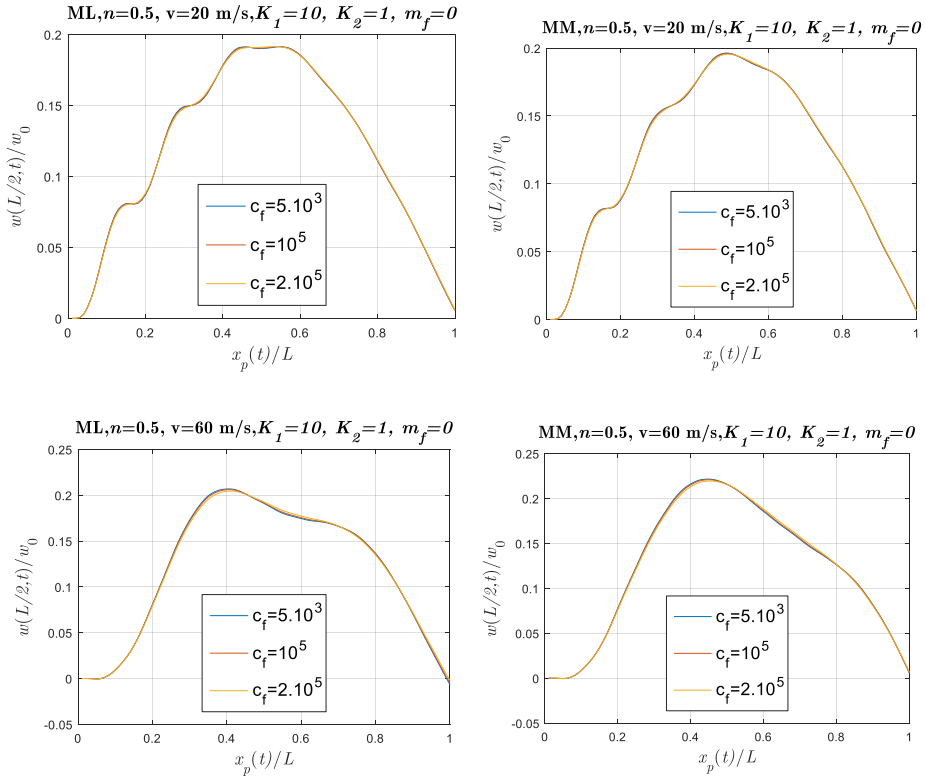

Figure 13. The midpoint response of the FGM beam for constant K_1=10, K_2=1, m_f=0, and various travelling velocities of the mass with v=20 and 60 m/s, and various foundation damping coefficients of c_f =5.10^3 and 2.10^5 Nsm^{-1}, and n=0.5

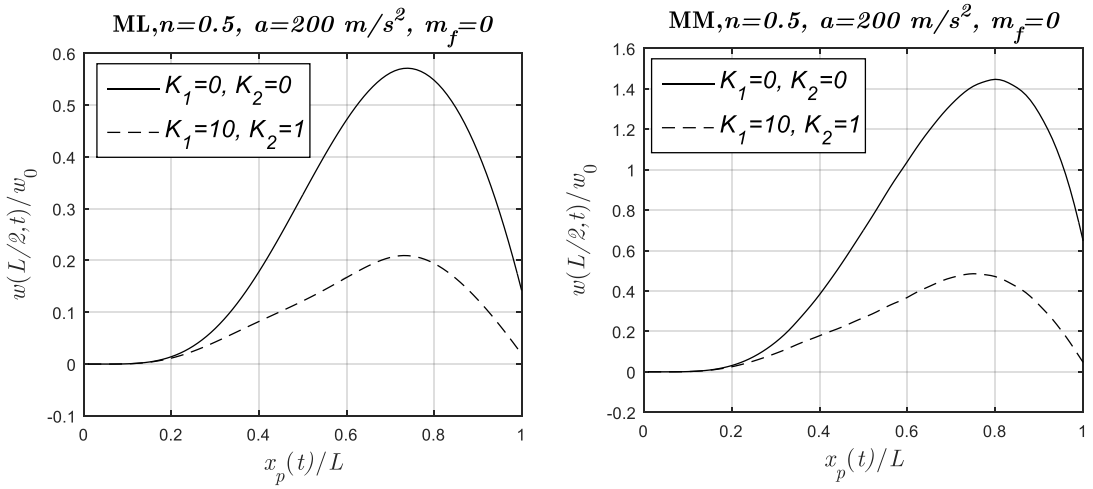

Figure 14. The midpoint responses in case of a sudden constant acceleration from 0 to 96.99 m/s with a acceleration of 200 m/s^2, n=0.5

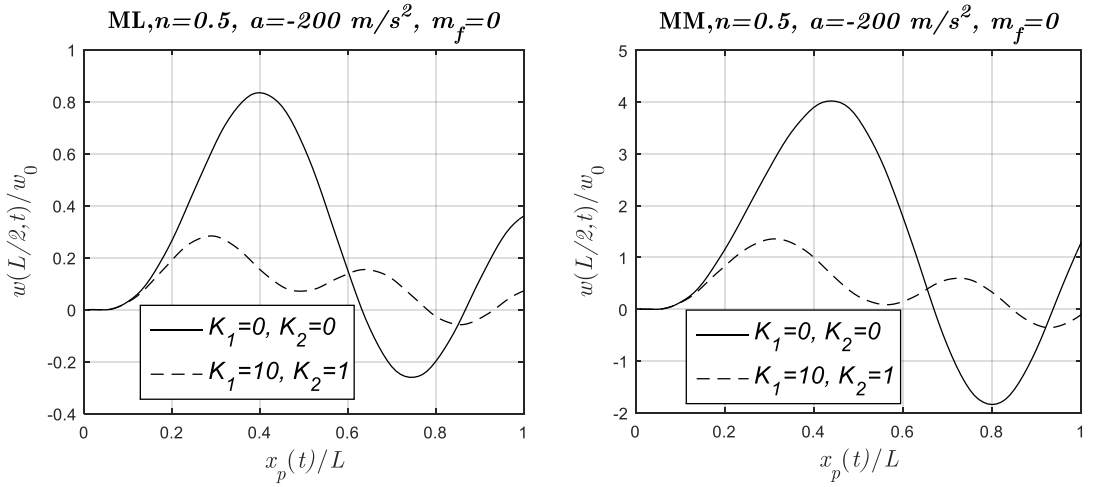

Figure 15. The midpoint responses in case of a sudden deceleration from 96.99 m/s to 0, with a constant deceleration of -200m/s^2, n=0.5.

5 Conclusions

In this article, under the excitation of an accelerating load the dynamics of a functionally graded Timoshenko beam supported by a four-parameter linear foundation is modelled using a modified FEM. From the results it can be stated that, in general, the maximum vibration amplitude of the whole system is governed by the actual natural frequencies and the excitation frequencies of the moving load. The excitation frequency of the moving load $\omega=\pi v/L$ is dependent to velocity and length L, but the natural frequencies of the beam-foundation system are dependent to many parameters of the system such as material, dimensions and boundary conditions, and parameters of the base including mass and viscous damping. In numerical results, every parameter that is effective on the frequency variation is investigated and discussed widely. In fact, the dynamic response depends on the variation of natural frequencies, so it is easy to predict the response when the actual natural frequency of the system and the excitation frequency of the mass are correctly defined or estimated.

In order to broaden the subject and provide a comprehensive perspective, the subject was discussed in detail by taking into account the moving mass and load and cases. And on the response of FGM

Timoshenko beam the effects of foundation parameters, material composition, mass velocity and mass inertia were presented.

In terms of computational simplicity, it is a common practice to ignore the effects of mass inertia in the literature for low-speed applications of the travelling loads. However, in this study, considering the higher speeds of the mass, the mass inertia is accounted in the modelling and analysis and the effects of it on the response of beam-base system extensively studied. Because the vibrations of the system under the effect of an accelerating mass can be analysed and computed considering the effect of each parameter of the foundation separately, using the method in this study, one can design a proper foundation system to satisfy the specified response limits for a special application of moving load. In the results of analysis, it is seen that the vibration frequency of the beam is quite variable depending of the location of the mass on the beam span for higher mass ratios if the parameters of the base are zero. However, it is also observed that level of the variation can be limited by inclusion of an appropriate base. When very large stiff foundation parameters are chosen the response approaches to the response of the static loading case due to increase in the natural frequencies at stiff foundations parameters. In high speed moving mass applications, the effect of the mass of the foundation appears to be obvious in the dynamic behaviour of the entire system. For this reason, it will be important for the accuracy of the calculations to consider the mass of the foundation in engineering calculations of current and future applications where vehicle speeds are gradually increasing.

References

[1] M.A. Koç, İ. Esen, Modelling and analysis of vehicle-structure-road coupled interaction considering structural flexibility , vehicle parameters and road roughness †, J. Mech. Sci. Technol. 31 (2017) 1–18. doi:10.1007/s12206-017-0913-y.

[2] M.A. Koc, I. Esen, H. Dal, Solution of the Moving Oscillator Problem using the Newmark ' s β Method, Int. J. Innov. Res. Sci. Eng. Technol. 5 (2016) 16–23.

[3] M.A. Koç, Finite Element and Numerical Vibration analysis of a Timoshenko and Euler-Bernoulli beams traversed by a moving high-speed train, J. Brazilian Soc. Mech. Sci. Eng. 7 (2021). doi:10.1007/s40430-021-02835-7.

[4] C. Mızrak, İ. Esen, The optimisation of rail vehicle bogie parameters with the fuzzy logic method in order to improve passenger comfort during passage over bridges, Int. J. Heavy Veh. Syst. 24 (2017) 113. doi:10.1504/IJHVS.2017.083057.

[5] İ. Esen, M.A. Koç, Dynamics of 35 mm anti-aircraft cannon barrel durig firing, in: Int. Symp. Comput. Sci. Eng., Aydın, 2013: pp. 252–257.

[6] İ. Esen, M.A. Koç, Optimization of a passive vibration absorber for a barrel using the genetic algorithm, Expert Syst. Appl. 42 (2015) 894–905. doi:10.1016/j.eswa.2014.08.038.

[7] M.A. Koç, İ. Esen, Y. Çay, Tip deflection determination of a barrel for the effect of an accelerating projectile before firing using finite element and artificial neural network combined algorithm, Lat. Am. J. Solids Struct. 13 (2016) 1968–1995. doi:http://dx.doi.org/10.1590/1679-78252718.

[8] M.A. Koç, I. Esen, Y. Çay, Dynamic analysis of gun barrel vibrations due to effect of an unbalanced projectile considering 2-D transverse displacements of barrel tip using a 3-D element technique, Lat. Am. J. Solids Struct. 15 (2018). doi:10.1590/1679-78254972.

[9] S.J. Singh, S.P. Harsha, Nonlinear dynamic analysis of sandwich S-FGM plate resting on pasternak foundation under thermal environment, Eur. J. Mech. - A/Solids. 76 (2019) 155–179. doi:https://doi.org/10.1016/j.euromechsol.2019.04.005.

[10] Q. Li, Q. Wang, D. Wu, X. Chen, Y. Yu, W. Gao, Geometrically nonlinear dynamic analysis of

organic solar cell resting on Winkler-Pasternak elastic foundation under thermal environment, Compos. Part B Eng. 163 (2019) 121–129. doi:https://doi.org/10.1016/j.compositesb.2018.11.022.

[11] M.T.A. Robinson, S. Adali, Buckling of nonuniform and axially functionally graded nonlocal Timoshenko nanobeams on Winkler-Pasternak foundation, Compos. Struct. 206 (2018) 95–103. doi:https://doi.org/10.1016/j.compstruct.2018.07.046.

[12] C.K. Rao, L.B. Rao, Torsional post-buckling of thin-walled open section clamped beam supported on Winkler-Pasternak foundation, Thin-Walled Struct. 116 (2017) 320–325. doi:https://doi.org/10.1016/j.tws.2017.03.017.

[13] D. Shahsavari, M. Shahsavari, L. Li, B. Karami, A novel quasi-3D hyperbolic theory for free vibration of FG plates with porosities resting on Winkler/Pasternak/Kerr foundation, Aerosp. Sci. Technol. 72 (2018) 134–149. doi:https://doi.org/10.1016/j.ast.2017.11.004.

[14] Q. Li, D. Wu, X. Chen, L. Liu, Y. Yu, W. Gao, Nonlinear vibration and dynamic buckling analyses of sandwich functionally graded porous plate with graphene platelet reinforcement resting on Winkler–Pasternak elastic foundation, Int. J. Mech. Sci. 148 (2018) 596–610. doi:https://doi.org/10.1016/j.ijmecsci.2018.09.020.

[15] F. Najafi, M.H. Shojaeefard, H.S. Googarchin, Nonlinear dynamic response of FGM beams with Winkler–Pasternak foundation subject to noncentral low velocity impact in thermal field, Compos. Struct. 167 (2017) 132–143. doi:https://doi.org/10.1016/j.compstruct.2017.01.063.

[16] K. Gao, W. Gao, D. Wu, C. Song, Nonlinear dynamic stability of the orthotropic functionally graded cylindrical shell surrounded by Winkler-Pasternak elastic foundation subjected to a linearly increasing load, J. Sound Vib. 415 (2018) 147–168. doi:https://doi.org/10.1016/j.jsv.2017.11.038.

[17] A. Deniz, Z. Zerin, Z. Karaca, Winkler-Pasternak foundation effect on the frequency parameter of FGM truncated conical shells in the framework of shear deformation theory, Compos. Part B Eng. 104 (2016) 57–70. doi:https://doi.org/10.1016/j.compositesb.2016.08.006.

[18] A.M. Zenkour, A.F. Radwan, Compressive study of functionally graded plates resting on Winkler–Pasternak foundations under various boundary conditions using hyperbolic shear deformation theory, Arch. Civ. Mech. Eng. 18 (2018) 645–658. doi:https://doi.org/10.1016/j.acme.2017.10.003.

[19] B. Mechab, I. Mechab, S. Benaissa, M. Ameri, B. Serier, Probabilistic analysis of effect of the porosities in functionally graded material nanoplate resting on Winkler–Pasternak elastic foundations, Appl. Math. Model. 40 (2016) 738–749. doi:https://doi.org/10.1016/j.apm.2015.09.093.

[20] J.K. Lee, S. Jeong, J. Lee, Natural frequencies for flexural and torsional vibrations of beams on Pasternak foundation, Soils Found. 54 (2014) 1202–1211. doi:https://doi.org/10.1016/j.sandf.2014.11.013.

[21] B. Akgöz, Ö. Civalek, Vibrational characteristics of embedded microbeams lying on a two-parameter elastic foundation in thermal environment, Compos. Part B Eng. 150 (2018) 68–77. doi:https://doi.org/10.1016/j.compositesb.2018.05.049.

[22] G. Chen, Z. Meng, D. Yang, Exact nonstationary responses of rectangular thin plate on Pasternak foundation excited by stochastic moving loads, J. Sound Vib. 412 (2018) 166–183. doi:https://doi.org/10.1016/j.jsv.2017.09.022.

[23] N.D. Duc, J. Lee, T. Nguyen-Thoi, P.T. Thang, Static response and free vibration of functionally graded carbon nanotube-reinforced composite rectangular plates resting on Winkler–Pasternak elastic foundations, Aerosp. Sci. Technol. 68 (2017) 391–402. doi:https://doi.org/10.1016/j.ast.2017.05.032.

[24] R.T. Corrêa, A.P. da Costa, F.M.F. Simões, Finite element modeling of a rail resting on a

Winkler-Coulomb foundation and subjected to a moving concentrated load, Int. J. Mech. Sci. 140 (2018) 432–445. doi:https://doi.org/10.1016/j.ijmecsci.2018.03.022.

[25] M.M. Keleshteri, H. Asadi, M.M. Aghdam, Nonlinear bending analysis of FG-CNTRC annular plates with variable thickness on elastic foundation, Thin-Walled Struct. 135 (2019) 453–462. doi:https://doi.org/10.1016/j.tws.2018.11.020.

[26] Y. Fan, Y. Xiang, H.-S. Shen, Nonlinear forced vibration of FG-GRC laminated plates resting on visco-Pasternak foundations, Compos. Struct. 209 (2019) 443–452. doi:https://doi.org/10.1016/j.compstruct.2018.10.084.

[27] F. Najafi, M.H. Shojaeefard, H.S. Googarchin, Nonlinear low-velocity impact response of functionally graded plate with nonlinear three-parameter elastic foundation in thermal field, Compos. Part B Eng. 107 (2016) 123–140. doi:https://doi.org/10.1016/j.compositesb.2016.09.070.

[28] R. Benferhat, T.H. Daouadji, M.S. Mansour, Free vibration analysis of FG plates resting on an elastic foundation and based on the neutral surface concept using higher-order shear deformation theory, Comptes Rendus Mécanique. 344 (2016) 631–641. doi:https://doi.org/10.1016/j.crme.2016.03.002.

[29] E. Bahmyari, M.R. Khedmati, Vibration analysis of nonhomogeneous moderately thick plates with point supports resting on Pasternak elastic foundation using element free Galerkin method, Eng. Anal. Bound. Elem. 37 (2013) 1212–1238. doi:https://doi.org/10.1016/j.enganabound.2013.05.003.

[30] R. Pavlovic, I. Pavlovic, Dynamic stability of Timoshenko beams on Pasternak viscoelastic foundation, Theor. Appl. Mech. i Primenj. Meh. 45 (2018) 67–81. doi:10.2298/tam171103005p.

[31] H. Ding, K.L. Shi, L.Q. Chen, S.P. Yang, Dynamic response of an infinite Timoshenko beam on a nonlinear viscoelastic foundation to a moving load, Nonlinear Dyn. 73 (2013) 285–298. doi:10.1007/s11071-013-0784-0.

[32] M.K. Ahmed, Natural frequencies and mode shapes of variable thickness elastic cylindrical shells resting on a Pasternak foundation, J. Vib. Control. 22 (2016) 37–50. doi:10.1177/1077546314528229.

[33] A.H. Sofiyev, On the buckling of composite conical shells resting on the Winkler–Pasternak elastic foundations under combined axial compression and external pressure, Compos. Struct. 113 (2014) 208–215. doi:10.1016/j.compstruct.2014.03.023.

[34] W.H. Lee, S.C. Han, W.T. Park, A refined higher order shear and normal deformation theory for E-, P-, and S-FGM plates on Pasternak elastic foundation, Compos. Struct. 122 (2015) 330–342. doi:10.1016/j.compstruct.2014.11.047.

[35] H. Matsunaga, Vibration and buckling of deep beam-columns on two-parameter elastic foundations, J. Sound Vib. 228 (1999) 359–376. doi:10.1006/jsvi.1999.2415.

[36] N.R. Naidu, G. V. Rao, Vibrations of initially stressed uniform beams on a two-parameter elastic foundation, Comput. Struct. (1995). doi:10.1016/0045-7949(95)00090-4.

[37] H.P. Lee, Dynamic Response of a Timoshenko Beam on a Winkler Foundation Subjected to a Moving Mass, Appl. Acoust. 55 (1998) 203–215. doi:10.1016/S0003-682X(97)00097-2.

[38] S.C. Dutta, R. Roy, A critical review on idealization and modeling for interaction among soil-foundation-structure system, Comput. Struct. 80 (2002) 1579–1594. doi:10.1016/S0045-7949(02)00115-3.

[39] A.D. Senalp, A. Arikoglu, I. Ozkol, V.Z. Dogan, Dynamic response of a finite length euler-bernoulli beam on linear and nonlinear viscoelastic foundations to a concentrated moving force, J. Mech. Sci. Technol. 24 (2010) 1957–1961. doi:10.1007/s12206-010-0704-x.

[40] M.H. Kargarnovin, D. Younesian, D.J. Thompson, C.J.C. Jones, Response of beams on nonlinear

viscoelastic foundations to harmonic moving loads, Comput. Struct. 83 (2005) 1865–1877. doi:10.1016/j.compstruc.2005.03.003.

[41] W. Luo, Y. Xia, S. Weng, Vibration of Timoshenko beam on hysteretically damped elastic foundation subjected to moving load, Sci. China Physics, Mech. Astron. 58 (2015) 84601. doi:10.1007/s11433-015-5664-9.

[42] M. Seguini, D. Nedjar, Nonlinear Analysis of Deep Beam Resting on Linear and Nonlinear Random Soil, Arab. J. Sci. Eng. 42 (2017) 3875–3893. doi:10.1007/s13369-017-2449-7.

[43] İ. Esen, M.A. Koç, Y. Çay, Finite element formulation and analysis of a functionally graded timoshenko beam subjected to an accelerating mass including inertial effects of the mass, Lat. Am. J. Solids Struct. 15 (2018) 1–18. doi:10.1590/1679-78255102.

[44] Y.H. Chen, Y.H. Huang, C.T. Shih, Response of an infinite tomoshenko beam on a viscoelastic foundation to a harmonic moving load, J. Sound Vib. 241 (2001) 809–824. doi:10.1006/jsvi.2000.3333.

[45] S.C. Mohanty, R.R. Dash, T. Rout, Static and dynamic analysis of a functionally graded Timoshenko beam on Winkler's elastic foundation, J. Eng. Res. Stud. 1 (2010) 149–165.

[46] S.C. Mohanty, R.R. Dash, T. Rout, Parametric instability of a functionally graded Timoshenko beam on Winkler's elastic foundation, Nucl. Eng. Des. 241 (2011) 2698–2715. doi:10.1016/j.nucengdes.2011.05.040.

[47] S.-H. Ju, H.-T. Lin, A finite element model of vehicle–bridge interaction considering braking and acceleration, J. Sound Vib. 303 (2007) 46–57. doi:https://doi.org/10.1016/j.jsv.2006.11.034.

[48] P.O. Azimi H, Galal K, A numerical element for vehicle-bridge interaction analysis of vehicles experiencing sudden deceleration., Eng Struct. 49 (2013) 792–805.

[49] D.K. NGUYEN, B.S. GAN, T.H. LE, Dynamic Response of Non-Uniform Functionally Graded Beams Subjected to a Variable Speed Moving Load, J. Comput. Sci. Technol. (2013). doi:10.1299/jcst.7.12.

[50] M. Şimşek, T. Kocatürk, Free and forced vibration of a functionally graded beam subjected to a concentrated moving harmonic load, Compos. Struct. 90 (2009) 465–473. doi:10.1016/j.compstruct.2009.04.024.

[51] S.M.R. Khalili, A.A. Jafari, S.A. Eftekhari, A mixed Ritz-DQ method for forced vibration of functionally graded beams carrying moving loads, Compos. Struct. 92 (2010) 2497–2511. doi:https://doi.org/10.1016/j.compstruct.2010.02.012.

[52] S.R. Mohebpour, P. Malekzadeh, A.A. Ahmadzadeh, Dynamic analysis of laminated composite plates subjected to a moving oscillator by FEM, Compos. Struct. (2011). doi:10.1016/j.compstruct.2011.01.003.

[53] J.-J. Wu, Transverse and longitudinal vibrations of a frame structure due to a moving trolley and the hoisted object using moving finite element, Int. J. Mech. Sci. 50 (2008) 613–625. doi:https://doi.org/10.1016/j.ijmecsci.2008.02.001.

[54] I. Esen, A new finite element for transverse vibration of rectangular thin plates under a moving mass, Finite Elem. Anal. Des. 66 (2013) 26–35. doi:10.1016/j.finel.2012.11.005.

[55] G.T. Michaltsos, A.N. Kounadis, The Effects of Centripetal and Coriolis Forces on the Dynamic Response of Light Bridges Under Moving Loads, J. Vib. Control. 7 (2001) 315–326. doi:10.1177/107754630100700301.

[56] İ. Esen, A new FEM procedure for transverse and longitudinal vibration analysis of thin rectangular plates subjected to a variable velocity moving load along an arbitrary trajectory, Lat. Am. J. Solids Struct. 12 (2015) 808–830.

[57] I. Esen, A modified FEM for transverse and lateral vibration analysis of thin beams under a mass moving with a variable acceleration, Lat. Am. J. Solids Struct. 14 (2017). doi:10.1590/1679-

78253180.

[58] H.P. Lee, Transverse vibration of a Timoshenko beam acted on by an accelerating mass, Appl. Acoust. 47 (1996) 319–330. doi:10.1016/0003-682X(95)00067-J.

[59] J.-H. Kim, G.H. Paulino, Finite element evaluation of mixed mode stress intensity factors in functionally graded materials, Int. J. Numer. Methods Eng. 53 (2002) 1903–1935. doi:10.1002/nme.364.

[60] P.J.W. Markworth AJ, Ramesh KS, Modelling studies applied to functionally graded materials, J. Mater. Sci. 30 (1995) 2183–2193.

[61] N.M. Wakashima K, Hirano T, Space applications of advanced structural materials, ESA, 1990.

[62] M.F. Eltaher MA, Alshorbagy AE, Determination of neutral axis position and its effect on natural frequencies of functionally graded macro/nanobeams, Compos Struct. 99 (2013) 193–201.

[63] D.-G. Zhang, Y.-H. Zhou, A theoretical analysis of FGM thin plates based on physical neutral surface, Comput. Mater. Sci. 44 (2008) 716–720. doi:10.1016/J.COMMATSCI.2008.05.016.

[64] J. Kosmatka, An improve two-node finite element for stability and natural frequencies of axial-loaded Timoshenko beams., Comput. Struct. 57 (1995) 141–149.

[65] A. Chakraborty, S. Gopalakrishnan, J.N. Reddy, A new beam finite element for the analysis of functionally graded materials, Int. J. Mech. Sci. (2003). doi:10.1016/S0020-7403(03)00058-4.

[66] S.A. Sina, H.M. Navazi, H. Haddadpour, An analytical method for free vibration analysis of functionally graded beams, Mater. Des. 30 (2009) 741–747. doi:10.1016/J.MATDES.2008.05.015.

[67] C. Zhang, A. Savaidis, G. Savaidis, H. Zhu, Transient dynamic analysis of a cracked functionally graded material by a BIEM, Comput. Mater. Sci. 26 (2003) 167–174. doi:https://doi.org/10.1016/S0927-0256(02)00395-6.

[68] L. Fryba, Vibration solids and structures under moving loads, Thomas Telford House, 1999.

If you are using any reference manager (e.g. Mendeley, Zotero Endnote etc), you may select standard style *IEEE or APA style.*